

Table 2
Nucleotide changes and amino acid substitutions in the cytopathic JFH1 subclone

Nucleotide ^a	Amino acid ^a
A1353G	M334V
C2842A	T843K
G3402A	G1017S
A5819G	Synonymous
T7662A	C2438S
C9153T	P2934S
G9232A	G2960D
G9293C	Synonymous
G9295C	R2985P
C9353A	H3000Q
G9355A	S3001N

^a Nucleotide and amino acid numbers were derived from pJFH1 full (Wakita et al., 2005).

host cell lines, detection of HCV-infected cells commonly relied on visualization of the infected focus by immunostaining HCV proteins (Zhong et al., 2005). Disadvantages include the costs of the antibodies and substrate, additional steps for assay and detection, and microscopic examination to count the foci. By using a highly permissive host cell line and optimizing several conditions, we have developed a plaque assay for HCV. Because the HCV-JFH1 strain is not absolutely cytopathic and does not kill all infected cells, the calculated plaque-forming units do not directly reflect HCV infectious titer but rather reflect cytopathogenicity or the percentage of cytopathic clones in the total infectious foci.

The HCV plaque assay revealed that JFH1 infection and replication developed cytopathic and noncytopathic infectious cell foci (Fig. 3B). One would suspect that the different outcomes of HCV replication might be attributable to the clonal heterogeneity of the host cells. However, there are several pieces of evidence that the Huh-7.5.1 cell line, which we used as host, might be a homogenous cell line. Huh-7.5.1 is derived from parental Huh7 cells through two rounds of clonal selection for neomycin resistance that were dependent on permissiveness for the HCV subgenomic replicon (Blight et al., 2002; Zhong

et al., 2005). Sumpter et al. have reported that the HCV-permissive feature is due to mutational inactivation of RIG-I, a cytoplasmic double-stranded RNA sensor that induces type-I IFN production (Sumpter et al., 2005). This evidence suggests that the cytopathic HCV replication is attributable to virus factors, in particular, virus genomic alteration and not by clonal variation or evolution of the host cells.

Indeed, the isolation of the plaque-forming HCV subclones and inoculation onto naive cells showed significantly higher replication yields (Fig. 8) and more frequent development of cytopathic plaques (Table 1). These findings indicate that HCV-JFH1 has evolved into cytopathic and noncytopathic subclones. Our results are similar to BVDV infection. BVDV is divided into two biotypes, cytopathic (*cp*) and noncytopathic (*ncp*) strains. Most *cp* strains, which induce strong apoptotic cell death upon infection, develop from the *ncp* strains by RNA recombination such as insertion of cellular sequences, duplications and rearrangements, and deletions and lead to expression of the NS3 protein (Meyers and Thiel, 1996). Kummerer et al. have reported that other *cp* strain had point mutations in NS2 that enhanced cleavage of NS2/3 junction and NS3 production (Kummerer and Meyers, 2000). As for HCV, considering a rapid HCV replication cycle and the poor fidelity of the viral NS5B RNA-dependent RNA polymerase (RdRp) (Bartenschlager and Lohmann, 2000; Kato et al., 2005), evolution of sequence variants may well develop even after a transfection of cloned HCV-RNA. Very recently, *in vitro* permissive subclones of HCV genotype 1a, H77S stain, have been reported, which have five cell culture-adaptive mutations in the NS3, 4A, and 5A regions (Yi et al., 2007). In these clones, introduction of amino acid substitutions in the p7 and NS2 region enhanced production of the virion particles.

Interestingly, sequence analyses of a cytopathic HCV-JFH1 subclone (PI #1) identified six amino acid substitutions in the NS5B RdRp (Table 2). Three of the six mutations were redundantly appeared in other clones that were independently isolated from the plaques (Table 3). These findings make us speculate that these amino acid substitutions may affect the enzymatic activity of RdRp by altering tertiary structure of the

Table 3
Nucleotide changes and amino acid substitutions in the NS5B regions of the cytopathic JFH1 subclones

PI #1	#1-1	#1-2	#1-3	PI #2	PI #3	PI #4
T7662A (C2438S)	T7662A (C2438S)	T7662A (C2438S)	T7662A (C2438S)	T7662A (C2438S)	T7662A (C2438S) A7550C C7551A (N2470T)	T7623A (S2428T)
C9153T (P2934S)	C9153T (P2934S)	C9153T (P2934S)	C9153T (P2934S)	G9162T (V2941L)	C9153T (P2934S)	G8259C C8260G (A2640R)
G9232A (G2960D)				G9235A (R2965Q)	A9201T (I2954F)	
G9295C (R2985P)	G9295C (R2985P)		G9295C (R2985P)			
C9353A (H3000Q)	C9353A (H3000Q)					
G9355A (S3001N)	G9355A (S3001N)		G9355A (S3001N)			G9355A (S3001N)

Nucleotide and amino acid numbers were derived from pJFH1 full (Wakita et al., 2005).

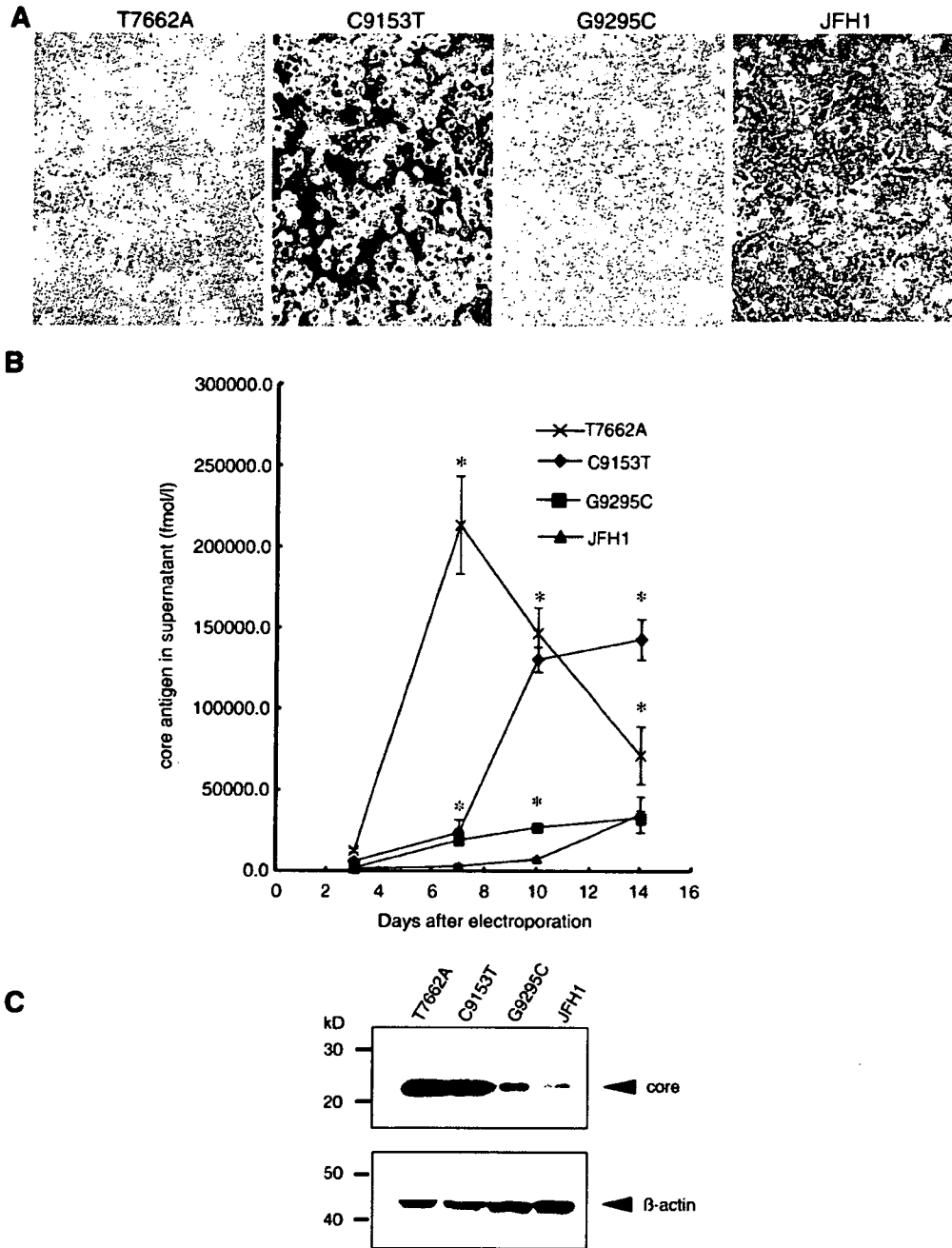


Fig. 9. Introduction of various mutations into the NS5B region of JFH1. The mutations identified in the cytopathic plaque PI #1; T7662A, C9153T, and G9295C were introduced individually into the parental JFH1. Each JFH1 mutant, T7662A, C9153T, and G9295C, RNA was transfected into Huh-7.5.1 cells by electroporation. The transfected cells were split every 3 to 5 days (see Materials and methods). (A) JFH1 mutants transfected Huh-7.5.1 cells were observed by phase-contrast microscopy at day 7 after transfection. (B) Levels of core antigen in the culture supernatants. The culture supernatants of transfected cells were collected on the days indicated, and the levels of core antigen were measured. Asterisks indicate *p*-values of less than 0.05. (C) The supernatants of JFH1 mutants transfected Huh-7.5.1 cells were transferred onto uninfected Huh-7.5.1 cells. The cells were harvested at 7 days after infection. Western blotting was performed using anti-core and anti-beta-actin.

thumb domain or affect the quaternary structure of the whole HCV replicase complex by altering surface affinity to other nonstructural proteins. Mapping of the amino acid substitutions in the RdRp tertiary structure has shown that the amino acid 2438 was located on the finger domain, and three amino acids,

2934, 2960, and 2985, were located on the outer surface of the thumb domain, which corresponds to the opposite side of the nucleotide tunnel. The other substitutions, 3000 and 3001, were within the domain of the polypeptide linking the polymerase to the membrane anchor (Lesburg et al., 1999). Very

recently, Zhong et al. have reported that long-term culture of HCV-JFH1 of more than 60 days leads to the evolution of certain mutations in the viral genome (Zhong et al., 2006). They identified amino acid changes in Core, E2, NS3, and NS5A regions, and especially E2 mutation increased infectivity and density changes of viruses. In our present study, however, we could not find those mutations in the virus subclones that we have isolated in the plaque assay technique. The discrepancy might be attributable to the presence or absence of HCV-CPE-induced cell clonal alteration of the host Huh-7.5.1 that occurs concomitantly with viral genetic evolution during long-term cell culture. Further analyses may be necessary to determine the most critical regions that regulate the viral replication efficiency and cytopathogenicity.

Interestingly, the mutant virus clones, T7662A (C2438S), C9153T (P2934S), and G9295C (R2985P), showed considerably higher replication efficiency and cytopathogenicity than the wild type JFH1 clone (Fig. 9). These results strongly suggest that certain NS5B mutations in the plaque-purified strains display more replication-efficient and cytopathic phenotypes. The present data are still preliminary. Further studies may be necessary to fully characterize these mutations and their functions, which include introduction of mutations of the HCV region and of the other plaque-purified viruses and combination of the mutations, and to study their effects on virus protein functions. We are at present analyzing derivative JFH1 clones in which other amino acid mutations were introduced.

Several clinical findings have suggested that HCV is not cytopathic and that antiviral immune responses such as cytotoxic T lymphocytes play important roles in HCV pathogenesis (Cerny and Chisari, 1999). On the other hand, apoptotic cell death is the first cellular response to many hepatotoxic events and has been implicated in the pathogenesis of liver diseases, such as viral hepatitis, autoimmune diseases, alcohol-induced injury, cholestasis, hepatocellular carcinoma, and fulminant hepatic failure (Canbay et al., 2004; Ghavami et al., 2005; Patel and Gores, 1995; Rodrigues et al., 2000; Rust and Gores, 2000; Thompson, 1995). Several clinical studies have shown that fulminant hepatic failure (FHF), from which HCV-JFH1 strain was isolated, showed far more hepatocyte apoptosis, as characterized by caspase activation and Fas-FasL expression, than chronic hepatitis and normal populations (Leifeld et al., 2006; Mita et al., 2005; Ryo et al., 2000). The ER stress markers GRP78 and ATF6 are upregulated in the HCV liver tissue as the histological grade advanced. In addition, GRP78 and ATF6 are upregulated as the histological grade increased in hepatocellular carcinoma (HCC) (Shuda et al., 2003) and proteomic analysis of HCC tissue samples has shown significant upregulation of HSP70 and GRP78 (Chuma et al., 2003; Takashima et al., 2003), indicating that these proteins may play important roles in HCV-induced hepatocarcinogenesis.

In conclusion, the cytopathic mutants of HCV-JFH1 strain were isolated by using plaque assay techniques. A mechanism of the cytopathic effects involved ER stress-mediated apoptosis that was triggered by virus infection. That process of cytopathic effects might explain one aspect of HCV-induced liver injury during acute infection. Further analyses of cellular effects on

HCV replication may elucidate the pathogenesis of HCV infection and may define novel host factors as targets of antiviral chemotherapeutics.

Materials and methods

Reagents

Recombinant human interferon alpha-2b was from Schering-Plough (Kenilworth, NJ). Beta-mercaptoethanol was from Wako (Osaka, Japan). Anti-CD81 antibody (JS-81) was from BD Biosciences (Franklin Lakes, NJ) (Morikawa et al., 2007).

Cells and cell culture

Huh-7.5.1 cells (Zhong et al., 2005) (kindly provided by Dr Francis V. Chisari) were maintained in Dulbecco's modified minimal essential medium (DMEM, Sigma) supplemented with 2 mmol/l L-glutamine and 10% fetal bovine serum at 37 °C under 5.0% CO₂.

In vitro RNA synthesis and transfection

A plasmid, pJFH1-full (Wakita et al., 2005), which encodes the full-length HCV-JFH1 sequence, and two control plasmids for pJFH1-full were used; pJFH1/GND that is a replication incompetent mutant with a mutation in the NS5B GDD motif and pJFH1/ΔE1-E2 in which a coding region of the HCV envelope proteins was deleted. The HCV RNA was synthesized using the RiboMax Large Scale RNA Production System (Promega, Madison, WI), with the linearized pJFH1 plasmid as template. After DNaseI (RQ-1 RNase-free DNase, Promega) treatment, the transcribed HCV-RNA was purified using ISOGEN (Nippon Gene, Tokyo, Japan). For the RNA transfection, Huh-7.5.1 cells were washed twice, and 5×10^6 cells were resuspended in Opti-MEM I (Invitrogen, Carlsbad, CA) containing 10 μg of HCV RNA, transferred into a 4-mm electroporation cuvette, and subjected to an electric pulse (1050 μF and 270 V) using the Easy Ject system (EquiBio, Middlessex, UK). After electroporation, the cell suspension was left for 5 min at room temperature and then incubated under normal culture conditions in a 10-cm diameter cell culture dish. The transfected cells were split every 3 to 5 days. The culture supernatants were subsequently transferred onto uninfected Huh-7.5.1 cells. The levels of HCV replication and viral protein expression were detected by real-time PCR, western blotting, and immunocytochemistry.

HCV subgenomic replicon constructs

HCV subgenomic replicon plasmid pRep-Feo was derived from the HCV-N strain pHCV1bneo-delS (Tanabe et al., 2004) and pSGR-JFH1 was from the HCV-JFH1 strain (Kato et al., 2003). The replicon RNA was synthesized from pRep-Feo or pSGR-JFH1 and transfected into Huh-7.5.1 cells. After culture in the presence of G418 (Wako), cell lines stably expressing the replicon were established.

Real-time RT-PCR analysis

Total cellular RNA was isolated using ISOGEN (Nippon Gene). Two micrograms of total cellular RNA was used to generate cDNA from each sample using SuperScript II (Invitrogen) reverse transcriptase. Expression of mRNA was quantified using Quanti Tect SYBR Green PCR Master Mix (QIAGEN, Valencia, CA) and the ABI 7500 Real-Time PCR System (Applied Biosystems, Foster City, CA). The primers used were as follows: HCV-JFH1 sense (positions 7090 to 7109; 5'-TCA GAC AGA GCC TGA GTC CA-3'), HCV-JFH1 antisense (positions 7404 to 7423; 5'-AGT TGC TGG AGG GCT TCT GA-3'), beta-actin sense (5'-ACA ATG AAG ATC AAG ATC ATT GCT CCT CCT-3'), and beta-actin antisense (5'-TTT GCG GTG GAC GAT GGA GGG GCC GGA CTC-3').

Quantification of HCV core antigen in the culture supernatant

The culture supernatants of JFH1-RNA transfected Huh-7.5.1 cells were collected on the days indicated, passed through a 0.45 µm filter (MILLEX-HA, Millipore, Bedford, MA), and stored at -80 °C. The levels of core antigen in the culture supernatants were measured using a chemiluminescence enzyme immunoassay (CLEIA) according to the manufacturer's protocol (Lumipulse Ortho HCV Antigen, Ortho-Clinical Diagnostics, Tokyo, Japan).

Western blotting

Western blotting was carried out as described previously (Tanabe et al., 2004; Yokota et al., 2003). Briefly, 10 µg of total cell lysate was separated by SDS-PAGE and blotted onto a polyvinylidene fluoride (PVDF) western blotting membrane. The membrane was incubated with the primary antibodies followed by a peroxidase-labeled anti-IgG antibody and visualized by chemiluminescence using the ECL western blotting Analysis System (Amersham Biosciences, Buckinghamshire, UK). The antibodies used were anti-core mouse monoclonal antibody 2H9 (provided by Dr. Wakita), anti-GRP78 goat monoclonal antibody, anti-GADD153/CHOP rabbit polyclonal antibody (Santa Cruz Biotechnology, Santa Cruz, CA), anti-eIF2-alpha, anti-phospho-eIF2-alpha rabbit polyclonal antibody (Cell Signaling, Danvers, CA), and anti-beta-actin antibody (Sigma).

Immunocytochemistry

HCV-JFH1-transfected or infected Huh-7.5.1 cells were cultured in Lab-Tek® Chamber Slide™ (Nalge Nunc International, Rochester, NY) or on 22-mm-round micro cover glasses (Matsunami, Tokyo, Japan). For detection of HCV-core and GRP78, cells were fixed with cold acetone for 15 min. The cells were incubated with the primary antibodies for 1 h at 37 °C and with Alexa Fluor 488 goat anti-mouse IgG antibody or Alexa Fluor 568 donkey anti-goat IgG antibody (Molecular Probes, Eugene, OR) for 1 h at room temperature. To analyze apoptosis of HCV-JFH1 infected cells, double staining for annexin V-FITC

binding and for cellular DNA using propidium iodide (PI) was performed using an annexin V-Fluorescein Staining Kit (Wako, Osaka, Japan). Cells were visualized by a fluorescence microscopy (BZ-8000, KEYENCE, Osaka, Japan).

Plaque assay

Huh-7.5.1 cells were seeded in collagen-coated 60-mm-diameter plates at a density of $2-4 \times 10^5$ cells per plates and were incubated at 37 °C under 5.0% CO₂ (as described above). After overnight incubation, HCV-infected culture supernatants were serially diluted in a final volume of 2 ml per plates and transferred onto the cell monolayers. After ~5 h of incubation, the inocula were removed, and the cell monolayers were overlaid with 8 ml of culture medium (DMEM, 2 mmol/l L-glutamine and 10% fetal bovine serum) that contained 0.8% methylcellulose. After 7 to 12 days of incubation under normal culture conditions, formation of cytopathic plaque was visualized by staining the cell monolayers with 0.08% crystal violet solution (Sigma). The levels of cytotoxicity were evaluated by counting the plaques and calculating the titer (PFU/ml). Similarly, the titers of infectivity were evaluated by performing immunocytochemistry to detect foci of HCV-core-positive cells and calculating the infectious focus-forming units (FFU/ml).

Sequence analyses

The cDNA from the isolated JFH1 plaque was amplified from cytopathic virus-infected Huh-7.5.1 cells by RT-PCR and subjected to direct sequence determination. Nucleotide sequences were read from both strands using Big Dye Terminator Cycle Sequencing Ready Reaction kits (Applied Biosystems) and an automated DNA sequencer (ABI PRISM® 310 Genetic Analyzer; Applied Biosystems).

Establishment of mutant JFH1 clones

In order to introduce various mutations into the NS5B region of JFH1, plasmid pJFH1 was digested with *Hind*III and the DNA fragment encompassing nt. 8231 to 9731 was subcloned into the pBluescriptII SK+ phagemid vector (Stratagene, La Jolla, CA). The following mutations were introduced into the DNA fragment in the subcloning vector by site-directed mutagenesis (Quick-ChangeII Site-Directed Mutagenesis Kit; Stratagene): C9153T and G9295C, respectively. Finally, these *Hind*III-*Hind*III fragments were subcloned back into the parental plasmid pJFH1. The mutation T7662A-introduced PCR fragment (nt. 7421–7839) was subcloned into the T-Vector (pGEM-T Easy Vector Systems; Promega) and digested with *Rsr*II and *Bsr*GI. Finally, these *Rsr*II-*Bsr*GI fragments were subcloned back into the parental plasmid.

Statistical analyses

Statistical analyses were performed using the Student's *t*-test, and *p*-values of less than 0.05 were considered as statistically significant.

Acknowledgments

We are indebted to Dr. Francis V. Chisari for providing the Huh-7.5.1 cell line. This study was supported by grants from the Japan Society for the Promotion of Science, Miyakawa Memorial Research Foundation, and Viral Hepatitis Research Foundation of Japan.

References

- Bartenschlager, R., Lohmann, V., 2000. Replication of hepatitis C virus. *J. Gen. Virol.* 81 (Pt 7), 1631–1648.
- Benali-Furet, N.L., Chami, M., Houel, L., De Giorgi, F., Vernejoul, F., Lagorce, D., Buscail, L., Bartenschlager, R., Ichas, F., Rizzuto, R., Paternini-Brechot, P., 2005. Hepatitis C virus core triggers apoptosis in liver cells by inducing ER stress and ER calcium depletion. *Oncogene* 24 (31), 4921–4933.
- Blight, K.J., Kolykhalov, A.A., Rice, C.M., 2000. Efficient initiation of HCV RNA replication in cell culture. *Science* 290 (5498), 1972–1974.
- Blight, K.J., McKeating, J.A., Rice, C.M., 2002. Highly permissive cell lines for subgenomic and genomic hepatitis C virus RNA replication. *J. Virol.* 76 (24), 13001–13014.
- Borisevich, V., Seregin, A., Nistler, R., Mutabazi, D., Yamshchikov, V., 2006. Biological properties of chimeric West Nile viruses. *Virology* 349 (2), 371–381.
- Canbay, A., Friedman, S., Gores, G.J., 2004. Apoptosis: the nexus of liver injury and fibrosis. *Hepatology* 39 (2), 273–278.
- Cerny, A., Chisari, F.V., 1999. Pathogenesis of chronic hepatitis C: immunological features of hepatic injury and viral persistence. *Hepatology* 30 (3), 595–601.
- Choukhi, A., Ung, S., Wychowski, C., Dubuisson, J., 1998. Involvement of endoplasmic reticulum chaperones in the folding of hepatitis C virus glycoproteins. *J. Virol.* 72 (5), 3851–3858.
- Chuma, M., Sakamoto, M., Yamazaki, K., Ohta, T., Ohki, M., Asaka, M., Hirohashi, S., 2003. Expression profiling in multistage hepatocarcinogenesis: identification of HSP70 as a molecular marker of early hepatocellular carcinoma. *Hepatology* 37 (1), 198–207.
- Despres, P., Frenkiel, M.P., Deubel, V., 1993. Differences between cell membrane fusion activities of two dengue type-1 isolates reflect modifications of viral structure. *Virology* 196 (1), 209–219.
- Despres, P., Flamand, M., Ceccaldi, P.E., Deubel, V., 1996. Human isolates of dengue type 1 virus induce apoptosis in mouse neuroblastoma cells. *J. Virol.* 70 (6), 4090–4096.
- Ferri, K.F., Kroemer, G., 2001. Organelle-specific initiation of cell death pathways. *Nat. Cell Biol.* 3 (11), E255–E263.
- Ghavami, S., Hashemi, M., Kadkhoda, K., Alavian, S.M., Bay, G.H., Los, M., 2005. Apoptosis in liver diseases—detection and therapeutic applications. *Med. Sci. Monit.* 11 (11), RA337–RA345.
- Gosert, R., Egger, D., Lohmann, V., Bartenschlager, R., Blum, H.E., Bienz, K., Moradpour, D., 2003. Identification of the hepatitis C virus RNA replication complex in Huh-7 cells harboring subgenomic replicons. *J. Virol.* 77 (9), 5487–5492.
- Harding, H.P., Zhang, Y., Ron, D., 1999. Protein translation and folding are coupled by an endoplasmic-reticulum-resident kinase. *Nature* 397 (6716), 271–274.
- He, B., 2006. Viruses, endoplasmic reticulum stress, and interferon responses. *Cell Death Differ.* 13 (3), 393–403.
- Hinshaw, V.S., Olsen, C.W., Dybdahl-Sissoko, N., Evans, D., 1994. Apoptosis: a mechanism of cell killing by influenza A and B viruses. *J. Virol.* 68 (6), 3667–3673.
- Jordan, R., Wang, L., Graczyk, T.M., Block, T.M., Romano, P.R., 2002. Replication of a cytopathic strain of bovine viral diarrhoea virus activates PERK and induces endoplasmic reticulum stress-mediated apoptosis of MDBK cells. *J. Virol.* 76 (19), 9588–9599.
- Kato, T., Furusaka, A., Miyamoto, M., Date, T., Yasui, K., Hiramoto, J., Nagayama, K., Tanaka, T., Wakita, T., 2001. Sequence analysis of hepatitis C virus isolated from a fulminant hepatitis patient. *J. Med. Virol.* 64 (3), 334–339.
- Kato, T., Date, T., Miyamoto, M., Furusaka, A., Tokushige, K., Mizokami, M., Wakita, T., 2003. Efficient replication of the genotype 2a hepatitis C virus subgenomic replicon. *Gastroenterology* 125 (6), 1808–1817.
- Kato, N., Nakamura, T., Dansako, H., Namba, K., Abe, K., Nozaki, A., Naka, K., Ikeda, M., Shimotohno, K., 2005. Genetic variation and dynamics of hepatitis C virus replicons in long-term cell culture. *J. Gen. Virol.* 86 (Pt 3), 645–656.
- Kaufman, R.J., 1999. Stress signaling from the lumen of the endoplasmic reticulum: coordination of gene transcriptional and translational controls. *Genes Dev.* 13 (10), 1211–1233.
- Koutsoudakis, G., Herrmann, E., Kallis, S., Bartenschlager, R., Pietschmann, T., 2007. The level of CD81 cell surface expression is a key determinant for productive entry of hepatitis C virus into host cells. *J. Virol.* 81 (2), 588–598.
- Kummerer, B.M., Meyers, G., 2000. Correlation between point mutations in NS2 and the viability and cytopathogenicity of Bovine viral diarrhoea virus strain Oregon analyzed with an infectious cDNA clone. *J. Virol.* 74 (1), 390–400.
- Leifeld, L., Nattermann, J., Fielenbach, M., Schmitz, V., Sauerbruch, T., Spengler, U., 2006. Intrahepatic activation of caspases in human fulminant hepatic failure. *Liver Int.* 26 (7), 872–879.
- Lesburg, C.A., Cable, M.B., Ferrari, E., Hong, Z., Mannarino, A.F., Weber, P.C., 1999. Crystal structure of the RNA-dependent RNA polymerase from hepatitis C virus reveals a fully encircled active site. *Nat. Struct. Biol.* 6 (10), 937–943.
- Lieberman, E., Fong, Y.L., Selby, M.J., Choo, Q.L., Cousens, L., Houghton, M., Yen, T.S., 1999. Activation of the gp78 and grp94 promoters by hepatitis C virus E2 envelope protein. *J. Virol.* 73 (5), 3718–3722.
- Lindenbach, B.D., Evans, M.J., Syder, A.J., Wolk, B., Tellinghuisen, T.L., Liu, C.C., Maruyama, T., Hynes, R.O., Burton, D.R., McKeating, J.A., Rice, C.M., 2005. Complete replication of hepatitis C virus in cell culture. *Science* 309 (5734), 623–626.
- Lohmann, V., Korner, F., Koch, J., Herian, U., Theilmann, L., Bartenschlager, R., 1999. Replication of subgenomic hepatitis C virus RNAs in a hepatoma cell line. *Science* 285 (5424), 110–113.
- Maekawa, S., Enomoto, N., Sakamoto, N., Kurosaki, M., Ueda, E., Kohashi, T., Watanabe, H., Chen, C.H., Yamashiro, T., Tanabe, Y., Kanazawa, N., Nakagawa, M., Sato, C., Watanabe, M., 2004. Introduction of NSSA mutations enables subgenomic HCV replicon derived from chimpanzee-infectious HC-J4 isolate to replicate efficiently in Huh-7 cells. *J. Viral Hepatitis* 11 (5), 394–403.
- Mendez, E., Ruggli, N., Collett, M.S., Rice, C.M., 1998. Infectious bovine viral diarrhoea virus (strain NADL) RNA from stable cDNA clones: a cellular insert determines NS3 production and viral cytopathogenicity. *J. Virol.* 72 (6), 4737–4745.
- Meyers, G., Thiel, H.J., 1996. Molecular characterization of pestiviruses. *Adv. Virus Res.* 47, 53–118.
- Mita, A., Hashikura, Y., Tagawa, Y., Nakayama, J., Kawakubo, M., Miyagawa, S., 2005. Expression of Fas ligand by hepatic macrophages in patients with fulminant hepatic failure. *Am. J. Gastroenterol.* 100 (11), 2551–2559.
- Mori, K., 2000. Tripartite management of unfolded proteins in the endoplasmic reticulum. *Cell* 101 (5), 451–454.
- Morikawa, K., Zhao, Z., Date, T., Miyamoto, M., Murayama, A., Akazawa, D., Tanabe, J., Sone, S., Wakita, T., 2007. The roles of CD81 and glycosaminoglycans in the adsorption and uptake of infectious HCV particles. *J. Med. Virol.* 79 (6), 714–723.
- Mottola, G., Cardinali, G., Ceccacci, A., Trozzi, C., Bartholomew, L., Torrisi, M.R., Pedrazzini, E., Bonatti, S., Migliaccio, G., 2002. Hepatitis C virus nonstructural proteins are localized in a modified endoplasmic reticulum of cells expressing viral subgenomic replicons. *Virology* 293 (1), 31–43.
- Munro, S., Pelham, H.R., 1986. An Hsp70-like protein in the ER: identity with the 78 kD glucose-regulated protein and immunoglobulin heavy chain binding protein. *Cell* 46 (2), 291–300.
- Nakagawa, M., Sakamoto, N., Tanabe, Y., Koyama, T., Itsui, Y., Takeda, Y., Chen, C.H., Kakinuma, S., Oooka, S., Maekawa, S., Enomoto, N., Watanabe, M., 2005. Suppression of hepatitis C virus replication by cyclosporin A is mediated by blockade of cyclophilins. *Gastroenterology* 129 (3), 1031–1041.
- Pahl, H.L., 1999. Signal transduction from the endoplasmic reticulum to the cell nucleus. *Physiol. Rev.* 79 (3), 683–701.

- Patel, T., Gores, G.J., 1995. Apoptosis and hepatobiliary disease. *Hepatology* 21 (6), 1725–1741.
- Pavio, N., Romano, P.R., Graczyk, T.M., Feinstone, S.M., Taylor, D.R., 2003. Protein synthesis and endoplasmic reticulum stress can be modulated by the hepatitis C virus envelope protein E2 through the eukaryotic initiation factor 2alpha kinase PERK. *J. Virol.* 77 (6), 3578–3585.
- Quaresma, J.A., Barros, V.L., Pagliari, C., Fernandes, E.R., Guedes, F., Takakura, C.F., Andrade Jr., H.F., Vasconcelos, P.F., Duarte, M.I., 2006. Revisiting the liver in human yellow fever: virus-induced apoptosis in hepatocytes associated with TGF-beta, TNF-alpha and NK cells activity. *Virology* 345 (1), 22–30.
- Rodrigues, C.M., Brites, D., Serejo, F., Costa, A., Ramalho, F., De Moura, M.C., 2000. Apoptotic cell death does not parallel other indicators of liver damage in chronic hepatitis C patients. *J. Viral Hepatitis* 7 (3), 175–183.
- Rust, C., Gores, G.J., 2000. Apoptosis and liver disease. *Am. J. Med.* 108 (7), 567–574.
- Ryo, K., Kamogawa, Y., Ikeda, I., Yamauchi, K., Yonehara, S., Nagata, S., Hayashi, N., 2000. Significance of Fas antigen-mediated apoptosis in human fulminant hepatic failure. *Am. J. Gastroenterol.* 95 (8), 2047–2055.
- Sato, H., Takimoto, T., Tanaka, S., Ogura, H., Shiraishi, K., Tanaka, J., 1989. Cytopathic effects induced by Epstein-Barr virus replication in epithelial nasopharyngeal carcinoma hybrid cells. *J. Virol.* 63 (8), 3555–3559.
- Shinoura, N., Yoshida, Y., Tsunoda, R., Ohashi, M., Zhang, W., Asai, A., Kirino, T., Hamada, H., 1999. Highly augmented cytopathic effect of a fiber-mutant E1B-defective adenovirus for gene therapy of gliomas. *Cancer Res.* 59 (14), 3411–3416.
- Shuda, M., Kondoh, N., Imazeki, N., Tanaka, K., Okada, T., Mori, K., Hada, A., Arai, M., Wakatsuki, T., Matsubara, O., Yamamoto, N., Yamamoto, M., 2003. Activation of the ATF6, XBP1 and grp78 genes in human hepatocellular carcinoma: a possible involvement of the ER stress pathway in hepatocarcinogenesis. *J. Hepatol.* 38 (5), 605–614.
- Su, H.L., Liao, C.L., Lin, Y.L., 2002. Japanese encephalitis virus infection initiates endoplasmic reticulum stress and an unfolded protein response. *J. Virol.* 76 (9), 4162–4171.
- Sumpter Jr., R., Loo, Y.M., Foy, E., Li, K., Yoneyama, M., Fujita, T., Lemon, S.M., Gale Jr., M., 2005. Regulating intracellular antiviral defense and permissiveness to hepatitis C virus RNA replication through a cellular RNA helicase, RIG-I. *J. Virol.* 79 (5), 2689–2699.
- Takashima, M., Kuramitsu, Y., Yokoyama, Y., Iizuka, N., Toda, T., Sakaida, I., Okita, K., Oka, M., Nakamura, K., 2003. Proteomic profiling of heat shock protein 70 family members as biomarkers for hepatitis C virus-related hepatocellular carcinoma. *Proteomics* 3 (12), 2487–2493.
- Tanabe, Y., Sakamoto, N., Enomoto, N., Kurosaki, M., Ueda, E., Maekawa, S., Yamashiro, T., Nakagawa, M., Chen, C.H., Kanazawa, N., Kakinuma, S., Watanabe, M., 2004. Synergistic inhibition of intracellular hepatitis C virus replication by combination of ribavirin and interferon-alpha. *J. Infect. Dis.* 189 (7), 1129–1139.
- Tardif, K.D., Mori, K., Siddiqui, A., 2002. Hepatitis C virus subgenomic replicons induce endoplasmic reticulum stress activating an intracellular signaling pathway. *J. Virol.* 76 (15), 7453–7459.
- Tardif, K.D., Mori, K., Kaufman, R.J., Siddiqui, A., 2004. Hepatitis C virus suppresses the IRE1-XBP1 pathway of the unfolded protein response. *J. Biol. Chem.* 279 (17), 17158–17164.
- Thompson, C.B., 1995. Apoptosis in the pathogenesis and treatment of disease. *Science* 267 (5203), 1456–1462.
- Vaughn, D.W., Hoke Jr., C.H., 1992. The epidemiology of Japanese encephalitis: prospects for prevention. *Epidemiol. Rev.* 14, 197–221.
- Wakita, T., Pietschmann, T., Kato, T., Date, T., Miyamoto, M., Zhao, Z., Murthy, K., Habermann, A., Krausslich, H.G., Mizokami, M., Bartenschlager, R., Liang, T.J., 2005. Production of infectious hepatitis C virus in tissue culture from a cloned viral genome. *Nat. Med.* 11 (7), 791–796.
- Waxman, L., Whitney, M., Pollok, B.A., Kuo, L.C., Darke, P.L., 2001. Host cell factor requirement for hepatitis C virus enzyme maturation. *Proc. Natl. Acad. Sci. U. S. A.* 98 (24), 13931–13935.
- Yanagiya, A., Jia, Q., Ohka, S., Horie, H., Nomoto, A., 2005. Blockade of the poliovirus-induced cytopathic effect in neural cells by monoclonal antibody against poliovirus or the human poliovirus receptor. *J. Virol.* 79 (3), 1523–1532.
- Yi, M., Ma, Y., Yates, J., Lemon, S.M., 2007. Compensatory mutations in E1, p7, NS2, and NS3 enhance yields of cell culture-infectious intergenotypic chimeric hepatitis C virus. *J. Virol.* 81 (2), 629–638.
- Yokota, T., Sakamoto, N., Enomoto, N., Tanabe, Y., Miyagishi, M., Maekawa, S., Yi, L., Kurosaki, M., Taira, K., Watanabe, M., Mizusawa, H., 2003. Inhibition of intracellular hepatitis C virus replication by synthetic and vector-derived small interfering RNAs. *EMBO Rep.* 4 (6), 602–608.
- Yu, C.Y., Hsu, Y.W., Liao, C.L., Lin, Y.L., 2006. Flavivirus infection activates the XBP1 pathway of the unfolded protein response to cope with endoplasmic reticulum stress. *J. Virol.* 80 (23), 11868–118680.
- Zheng, Y., Gao, B., Ye, L., Kong, L., Jing, W., Yang, X., Wu, Z., Ye, L., 2005. Hepatitis C virus non-structural protein NS4B can modulate an unfolded protein response. *J. Microbiol.* 43 (6), 529–536.
- Zhong, J., Gastaminza, P., Cheng, G., Kapadia, S., Kato, T., Burton, D.R., Wieland, S.F., Uprichard, S.L., Wakita, T., Chisari, F.V., 2005. Robust hepatitis C virus infection in vitro. *Proc. Natl. Acad. Sci. U. S. A.* 102 (26), 9294–9299.
- Zhong, J., Gastaminza, P., Chung, J., Stamataki, Z., Isogawa, M., Cheng, G., McKeating, J.A., Chisari, F.V., 2006. Persistent hepatitis C virus infection in vitro: coevolution of virus and host. *J. Virol.* 80 (22), 11082–11093.

DDX3 DEAD-Box RNA Helicase Is Required for Hepatitis C Virus RNA Replication[∇]

Yasuo Ariumi,¹ Misao Kuroki,¹ Ken-ichi Abe,¹ Hiromichi Dansako,¹ Masanori Ikeda,¹ Takaji Wakita,² and Nobuyuki Kato^{1*}

Department of Molecular Biology, Okayama University Graduate School of Medicine, Dentistry, and Pharmaceutical Sciences, 2-5-1, Shikata-cho, Okayama 700-8558,¹ and Department of Virology II, National Institute of Infectious Diseases, Toyama 1-23-1, Shinjuku-ku, Tokyo 162-8640,² Japan

Received 11 July 2007/Accepted 5 September 2007

DDX3, a DEAD-box RNA helicase, binds to the hepatitis C virus (HCV) core protein. However, the role(s) of DDX3 in HCV replication is still not understood. Here we demonstrate that the accumulation of both genome-length HCV RNA (HCV-O, genotype 1b) and its replicon RNA were significantly suppressed in HuH-7-derived cells expressing short hairpin RNA targeted to DDX3 by lentivirus vector transduction. As well, RNA replication of JFH1 (genotype 2a) and release of the core into the culture supernatants were suppressed in DDX3 knockdown cells after inoculation of the cell culture-generated HCvc. Thus, DDX3 is required for HCV RNA replication.

DEAD-box RNA helicases are involved in various RNA metabolic processes, including transcription, translation, RNA splicing, RNA transport, and RNA degradation (9, 20). DDX1 and DDX3, DEAD-box RNA helicases, have been implicated in the replication of human immunodeficiency virus type 1 (HIV-1). Both DDX1 and DDX3 interact with HIV-1 Rev and enhance Rev-dependent HIV-1 RNA nuclear export (10, 24).

On the other hand, DDX3 binds to the hepatitis C virus (HCV) core protein (17, 19, 25), and DDX3 expression is deregulated in HCV-associated hepatocellular carcinoma (HCC) (7, 8). However, the biological function of DDX3 in HCV replication is still not understood. To address this issue, we first used lentivirus vector-mediated RNA interference to stably knock down DDX3 in three HuH-7-derived cell lines: O cells, harboring a replicative genome-length HCV RNA (HCV-O, genotype 1b) (13); sO cells, harboring its subgenomic replicon of HCV RNA (14); or RSc cured cells, which cell culture-generated HCV (HCvc) (JFH1, genotype 2a) (23) could infect and effectively replicate in (M. Ikeda et al., unpublished data). Oligonucleotides with the following sense and antisense sequences were used for the cloning of short hairpin RNA (shRNA)-encoding sequences against DDX3 in the lentivirus vector: for DDX3i#3, 5'-GATCCCCGGAGGA AATTATAACTCCCTTCAAGAGAGGGAGTTATAATTT CCTCCTTTTTGGAAA-3' (sense) and 5'-AGCTTTTCCAA AAAGGAGGAAATTATAACTCCCTCTTGAAGGGA GTTATAATTTCTCCGGG-3' (antisense); for DDX3i#7, 5'-GATCCCCGGTACCCTGCCAAACAAGTTCAAGAG ACTTGTGGCAGGGTGACCTTTTTGGAAA-3' (sense) and 5'-AGCTTTTCCAAAAGGTACCCTGCCAAACAA

GTCTCTTGAAGTTGTTTGGCAGGGTGACCGGG-3' (antisense). These oligonucleotides were annealed and subcloned into the BglII-HindIII site, downstream from an RNA polymerase III promoter of pSUPER (6). To construct pLV-DDX3i#3 and pLV-DDX3i#7, the BamHI-SalI fragments of the corresponding pSUPER plasmids were subcloned into the BamHI-SalI site of pRDI292 (5), an HIV-1-derived self-inactivating lentivirus vector containing a puromycin resistance marker allowing for the selection of transduced cells. The vesicular stomatitis virus G protein (VSV-G)-pseudotyped HIV-1-based vector system has been described previously (18). We used the second-generation packaging construct pCMV-ΔR8.91 (26) and the VSV-G-envelope plasmid pMDG2. The lentivirus vector particles were produced by transient transfection of 293FT cells with FuGene 6 (Roche).

Western blot analysis of the lysates demonstrated the only trace of DDX3 protein in DDX3 knockdown O cells (DDX3i#3) (Fig. 1A). In this context, the HCV core expression level was significantly decreased in the DDX3 knockdown O cells (Fig. 1A). To further confirm this finding, we examined the level of HCV RNA in these cells. We found that accumulation of genome-length HCV-O RNA was notably suppressed in DDX3 knockdown O cells (Fig. 1B). Furthermore, the efficiency of colony formation in DDX3 knockdown O cells (created by eliminating genome-length HCV RNA from O cells by interferon treatment) transfected with the genome-length HCV-O RNA with an adapted mutation at amino acid (aa) position 1609 in the NS3 helicase region (K1609E) (13) was also notably reduced compared with that in control cells (Fig. 1C). In contrast, highly efficient knockdown of an unrelated host factor, poly(ADP-ribose) polymerase 1 (PARP-1) (4), had no observable effects on HCV RNA replication, the efficiency of colony formation, or the core expression level (data not shown), suggesting that our finding was not due to a nonspecific event. Interestingly, accumulation of the subgenomic replicon RNA (HCV-sO) was also suppressed in DDX3 knockdown sO cells (Fig. 1D). Moreover, we examined the potential role of DDX3 in an HCV infection and produc-

* Corresponding author. Mailing address: Department of Molecular Biology, Okayama University Graduate School of Medicine, Dentistry, and Pharmaceutical Sciences, 2-5-1, Shikata-cho, Okayama 700-8558, Japan. Phone: 81 86 235 7386. Fax: 81 86 235 7392. E-mail: nkato@md.okayama-u.ac.jp.

[∇] Published ahead of print on 12 September 2007.

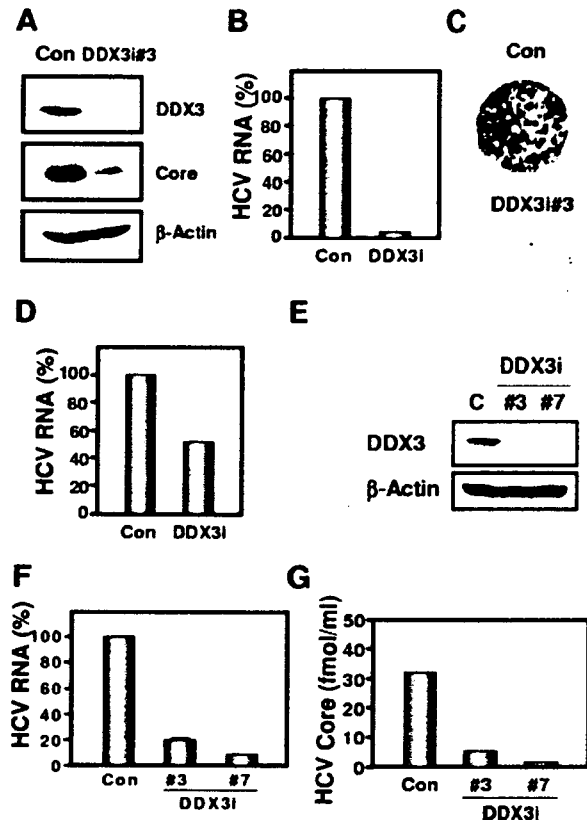


FIG. 1. Requirement of DDX3 for HCV replication. (A to D) Effect of DDX3 knockdown on HCV RNA replication. (A) Inhibition of DDX3 expression by shRNA-producing lentivirus vector. The results of Western blot analysis of cellular lysates with anti-DDX3 (ProSci), anti-HCV core (CP-9; Institute of Immunology), or an anti- β -actin antibody (Sigma) in O cells expressing shRNA against DDX3 (DDX3i#3) as well as in O cells transduced with a control lentivirus vector (Con) are shown. (B) The level of genome-length HCV RNA was monitored by real-time LightCycler PCR (Roche). Experiments were done in duplicate, and bars represent the mean percentages of HCV RNA. (C) Efficiency of colony formation in DDX3 knockdown cells. In vitro-transcribed ON/C-5B K1609E RNA (2 μ g) was transfected into the DDX3 knockdown O cells (DDX3i#3) or the O cells transduced with a control lentivirus vector (Con). G418-resistant colonies were stained with Coomassie brilliant blue at 3 weeks after electroporation of RNA. Experiments were done in duplicate, and representative results are shown. (D) The level of subgenomic replicon RNA was monitored by real-time LightCycler PCR. Experiments were done in duplicate, and bars represent the mean percentages of HCV RNA. (E to G) Effect of DDX3 knockdown on HCV infection. (E) Inhibition of DDX3 expression by shRNA-producing lentivirus vector. The results of Western blot analysis of cellular lysates with anti-DDX3 or an anti- β -actin antibody for RSc cells expressing the shRNA DDX3i#3 or DDX3i#7 and for RSc cells transduced with a control lentivirus vector (Con) are shown. (F) The level of genome-length HCV (JFH1) RNA was monitored by real-time LightCycler PCR after inoculation of the cell culture-generated HCVcc. Results from three independent experiments are shown. (G) The levels of the HCV core in the culture supernatants were determined by an enzyme-linked immunosorbent assay (Mitsubishi Kagaku Bio-Clinical Laboratories). Experiments were done in duplicate, and bars represent the mean HCV core protein levels.

tion system (23). We found 80 to 90% reductions in the accumulation of JFH1 RNA and 82 to 94% reductions in the release of the core into the culture supernatants in DDX3 knockdown HuH-7-derived RSc cured cells at 4 days after

inoculation of HCVcc (Fig. 1E to G). Thus, DDX3 seems to be required for HCV RNA replication.

Previously, DDX3 was identified as an HCV core-interacting protein by yeast two-hybrid screening. This interaction required the N-terminal domain of the core (aa 1 to 59) and the C-terminal domain of DDX3 (aa 553 to 622) (17, 19, 25). To determine whether the core can interact with DDX3 regardless of the HCV genotype, we used the HCV-O core (genotype 1b) and the JFH1 core (genotype 2a) (Table 1). We first examined their subcellular localization by confocal laser scanning microscopy as previously described (3). Consistent with previous reports (17, 19, 25), both the HCV-O core and JFH1 core mostly colocalized with DDX3 in the perinuclear region (Fig. 2A). Then we immunoprecipitated lysates from 293FT cells in which hemagglutinin (HA)-tagged DDX3 and HCV-O core, JFH1 core, or their 40-aa N-truncated mutants were overexpressed with an anti-HA antibody. Cells were lysed in a buffer containing 50 mM Tris-HCl (pH 8.0), 150 mM NaCl, 4 mM EDTA, 0.5% NP-40, 10 mM NaF, 0.1 mM Na_3VO_4 , 1 mM dithiothreitol, and 1 mM phenylmethylsulfonyl fluoride. Lysates were precleared with 30 μ l of protein G-Sepharose (GE Healthcare Bio-Sciences). Precleared supernatants were incubated with 1 μ g of anti-HA antibody (3F10; Roche) at 4°C for 1 h. Following absorption of the precipitates

TABLE 1. Primers used for construction of the HCV core-expressing plasmids^a

Plasmid name	Direction	Primer sequence
pCXbsr/core(HCV-O)	Forward	5'-GGAATCCACCATGAG CACGAATCCTAAACCTC-3
	Reverse	5'-ATAAGAATGCGGCCGC TATCAAGCGGAAGCTGG GATGGT-3'
pcDNA3/core(HCV-O)	Forward	5'-CGGGATCCAAGATGAGC ACGAATCCTAAACCTCAA AGA-3'
	Reverse	5'-CCGCTCGAGTCAAGCGG AAGCTGGGATGGTCAAA CA-3'
pcDNA3/ Δ core(HCV-O)	Forward	5'-CGGGATCCAAGATGGGC CCCAGGTTGGGTGTGCG C-3'
	Reverse	5'-CCGCTCGAGTCAAGCGG AAGCTGGGATGGTCAAA CA-3'
pcDNA3/core(JFH1)	Forward	5'-CGGGATCCAAGATGAGC ACAAATCCTAAACCTCAA AGA-3'
	Reverse	5'-CCGCTCGAGTCAAGCAG AGACCGGAACGGTGTATG CA-3'
pcDNA3/ Δ core(JFH1)	Forward	5'-CGGGATCCAAGATGGGC CCCAGGTTGGGTGTGCG C-3'
	Reverse	5'-CCGCTCGAGTCAAGCAG AGACCGGAACGGTGTATG CA-3'

^a To construct pCXbsr/core(HCV-O), a DNA fragment encoding the core was amplified by PCR from pON/C-5B (13) with the indicated primers. The PCR product was digested with EcoRI-NotI and subcloned into the same site of pCX4bsr (1). To construct pcDNA3/core(HCV-O), pcDNA3/FLAG-core(HCV-O), pcDNA3/ Δ core(HCV-O), and pcDNA3/FLAG- Δ core(HCV-O), DNA fragments encoding the core were amplified by PCR from pON/C-5B (13) with the indicated primer sets. To construct pcDNA3/core(JFH1), pcDNA3/FLAG-core(JFH1), pcDNA3/ Δ core(JFH1), and pcDNA3/FLAG- Δ core(JFH1), DNA fragments encoding the core were amplified by PCR from pJFH1 (23) with the indicated primer sets. The PCR products were digested with BamHI and XhoI and then subcloned into the same site of pcDNA3 (Invitrogen) or pcDNA3-FLAG (2).

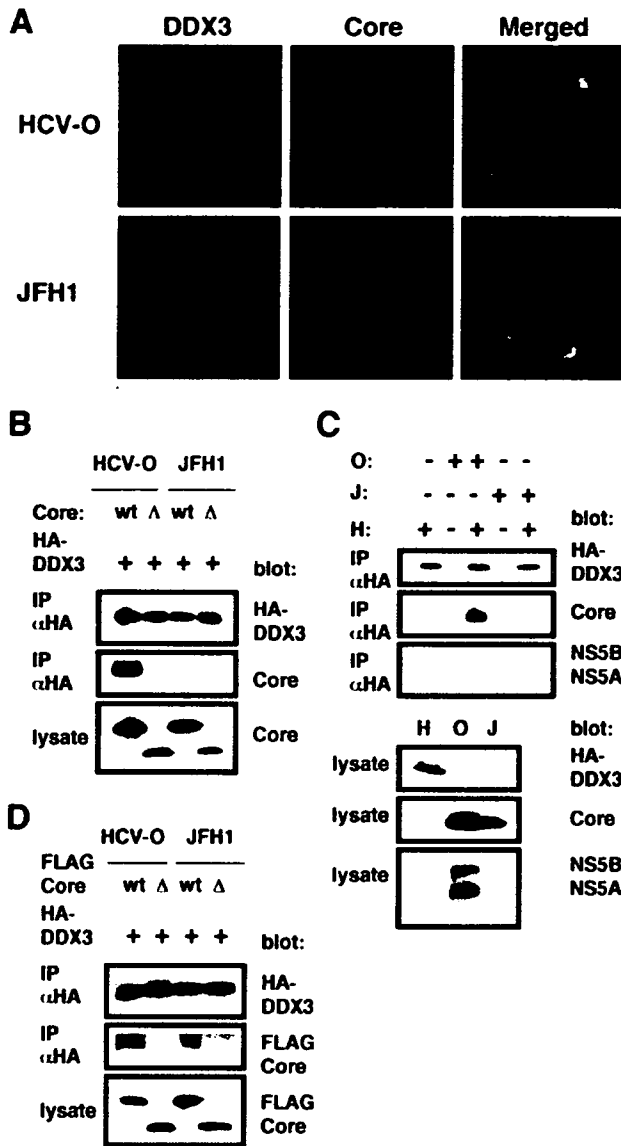


FIG. 2. Interaction of the HCV core with DDX3. (A) The HCV core colocalizes with DDX3. 293FT cells cotransfected with 100 ng of pCXbsr/core(HCV-O) or pcDNA3/core(JFH1) and 200 ng of pHA-DDX3 were examined by confocal laser scanning microscopy. Cells were stained with anti-HCV core (CP-9 and CP-11 mixture) and anti-DDX3 antibodies and were then visualized with fluorescein isothiocyanate (DDX3) or Cy3 (core). Images were visualized using confocal laser scanning microscopy (LSM510; Carl Zeiss). The right panels exhibit the two-color overlay images (Merged). Colocalization is shown in yellow. (B) The core binds to DDX3. 293FT cells were cotransfected with 4 μg of pHA-DDX3 and 4 μg of pCXbsr/core(HCV-O) (wt), pcDNA3/Δcore(HCV-O) (Δ), pcDNA3/core(JFH1) (wt), or pcDNA3/Δcore(JFH1) (Δ). The cell lysates were immunoprecipitated with an anti-HA antibody (3F10; Roche), followed by immunoblot analysis using either anti-HA (HA-7; Sigma) or anti-HCV core antibody (CP-9 and CP-11 mixture). (C) 293FT cells transfected with 4 μg of pHA-DDX3 (H), O cells (O), or RSc cells 3 days after inoculation of HCVcc (JFH1) (J) were lysed and immunoprecipitated (IP) with 1 μg of anti-HA antibody (3F10), followed by immunoblotting with anti-HA (HA-7), anti-core (CP-9 and CP-11 mixture), or anti-HCV NS5A (no. 8926) and anti-HCV NS5B. (D) 293FT cells transfected with 4 μg of pHA-DDX3 and 4 μg of pcDNA3/FLAG-core(HCV-O) (wt), pcDNA3/FLAG-Δcore(HCV-O) (Δ), pcDNA3/FLAG-core(JFH1) (wt), or

on 30 μl of protein G-Sepharose resin for 1 h, the resin was washed four times with 700 μl lysis buffer. Proteins were eluted by boiling the resin for 5 min in 1× Laemmli sample buffer. The proteins were then subjected to sodium dodecyl sulfate-polyacrylamide gel electrophoresis, followed by immunoblot analysis using either anti-HA (HA-7; Sigma) or anti-HCV core antibody (CP-9 and CP-11 mixture). We observed that the HCV-O core but not its N-truncated mutant could strongly bind to HA-tagged DDX3 (Fig. 2B). In contrast, the binding activity of the JFH1 core to HA-tagged DDX3 seemed to be fairly weak (Fig. 2B). As well, immunoprecipitation of lysates of 293FT cells expressing HA-tagged DDX3, O cells, or JFH1-infected RSc cells, or mixtures of these lysates, with an anti-HA antibody revealed that HCV-O core but not JFH1 core could bind strongly to DDX3 (Fig. 2C). The anti-HCV core antibody we used could detect both HCV-O core and JFH1 core (Fig. 2), while both anti-HCV NS5A and anti-NS5B antibodies failed to detect JFH1 NS5A and NS5B (Fig. 2C). At least, we failed to detect an interaction between DDX3 and either HCV-O NS5A or NS5B under experimental conditions that permitted the core to interact with DDX3 by immunoprecipitation (Fig. 2C). In contrast, the FLAG-tagged JFH1 core could bind to HA-tagged DDX3 just as efficiently as the FLAG-tagged HCV-O core could (Fig. 2D). Thus, the binding affinity or stability of the complex formed between the JFH1 core and DDX3 might be weaker than that between the HCV-O core and DDX3.

Since DDX3 is required for HIV-1 and HCV replication, we hypothesized that the HCV core might affect the function of HIV-1 Rev when both proteins were coexpressed. To test this hypothesis, we used the Rev-dependent luciferase-based reporter plasmid pDM628, harboring a single intron that includes both the Rev-responsive element (RRE) and the luciferase coding sequences (Fig. 3A) (10). In this system, Rev binds to RRE on the unspliced reporter mRNA, allowing its export from the nucleus for luciferase reporter gene expression, while the intron containing the luciferase gene is excised during RNA splicing when cells are transiently transfected with pDM628 alone. As previously reported (10), the luciferase activity in 293FT cells transfected with this reporter plasmid was stimulated by Rev, which induced a fourfold increase in the reporter signal (Fig. 3B). Luciferase activity was increased eightfold by the combination of Rev and DDX3, whereas neither the HCV-O core nor the JFH1 core had any effect on this Rev function (Fig. 3B). Since the Rev-binding domain (the N-terminal domain) and the core-binding domain (the C-terminal domain) do not overlap in DDX3, the HCV core might not compete with HIV-1 Rev for binding with DDX3. However, the development of a novel DDX3 inhibitor might provide a powerful antiviral agent against both HIV-1 and HCV (15).

Taking these results together, this study has shown for the first time that DDX3 is required for HCV RNA replication.

pcDNA3/FLAG-Δcore(JFH1) (Δ) were lysed and immunoprecipitated with 1 μg of an anti-HA antibody (3F10), followed by immunoblotting with an anti-HA (HA-7) or anti-core (CP-9 and CP-11 mixture) antibody.

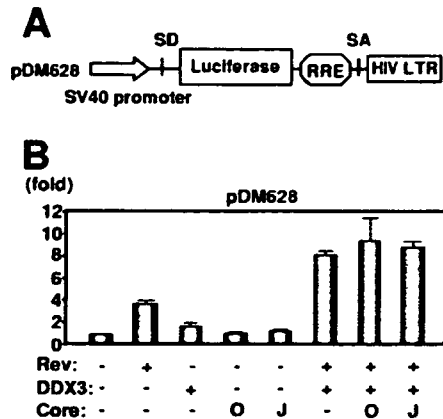


FIG. 3. HCV core does not affect the DDX3-mediated synergistic activation of Rev function. (A) Schematic representation of HIV-1 Rev-dependent luciferase-based reporter plasmid pDM628 harboring a splicing donor (SD), splicing acceptor (SA), and RRE. (B) 293FT cells were cotransfected with 100 ng of pDM628, 200 ng of pcRev, 200 ng of pHA-DDX3, and/or 100 ng of either pcDNA3/core(HCV-O) (O) or pcDNA3/core(JFH1) (J). A luciferase assay was performed 24 h later. All transfections utilized equal total amounts of plasmid DNA owing to the addition of the empty vector pcDNA3 to the transfection mixture. The relative stimulation of luciferase activity (*n*-fold) is shown. The results shown are means from three independent experiments.

Since helicases are motor enzymes that use energy derived from nucleoside triphosphate hydrolysis to unwind double-stranded nucleic acids, the DDX3-core complex might unwind the HCV double-stranded RNA and separate the RNA strands or might contribute to the function of HCV NS3 helicase. Since the replication of subgenomic replicon RNA was also partially suppressed in DDX3 knockdown cells (Fig. 1D), DDX3 might be associated with an HCV nonstructural protein(s) or HCV RNA itself. Indeed, Tingting et al. recently reported that DDX1 bound to both the HCV 3' untranslated region (3' UTR) and the HCV 5' UTR and that short interfering RNA-mediated knockdown of DDX1 caused a marked reduction in the replication of subgenomic replicon RNA (22). Furthermore, Goh et al. demonstrated that DDX5/p68 associated with HCV NS5B and that depletion of endogenous DDX5 correlated with a reduction in the transcription of negative-strand HCV RNA (11). However, we failed to observe an interaction between DDX3 and NS5A or NS5B by immunoprecipitation under our experimental conditions in which the core could interact with DDX3 (Fig. 2C). Importantly, our DDX3 knockdown study demonstrated a more significant reduction in the accumulation of genome-length HCV RNA (95% reduction) than in the accumulation of subgenomic replicon RNA (52% reduction) (Fig. 1B and D). To date, it has been demonstrated that the 5' UTR, the 3' UTR, and the NS3-to-NS5B coding region are sufficient for HCV RNA replication (16); however, the core might be partly involved in the replication of genome-length HCV RNA. Importantly, DDX1 and DDX3 were specifically detected in the lipid droplets of core-expressing Hep39 cells by proteomic analysis (21), suggesting that DDX3 might be associated with HCV assembly or might incorporate into the HCV virion through interaction with the core to act as an RNA chaperone.

Recent studies have suggested a potential role of DDX3 and DDX5 in the pathogenesis of HCV-related liver diseases. DDX3 expression is deregulated in HCV-associated HCC (7, 8), and Huang et al. identified single-nucleotide polymorphisms in the DDX5 gene that were significantly associated with an increased risk of advanced fibrosis in patients with chronic hepatitis C (12). Interestingly, DDX3 might be a candidate tumor suppressor. DDX3 inhibits colony formation in various cell lines, including HuH-7, and up-regulates the p21^{waf1/cip1} promoter (8). If DDX3 could in fact suppress tumor growth, then the core might overcome DDX3-mediated cell growth arrest and down-regulate p21^{waf1/cip1} through interaction with DDX3, and it might also be involved in HCC development.

We thank D. Trono, K.-T. Jeang, V. Yedavalli, R. J. Pomerantz, J. Fang, R. Iggo, M. Hijikata, T. Akagi, and M. Kohara for pCMVΔR8.91, pMDG2, pHA-DDX3, pDM628, pcRev, pSUPER, pRDI292, 293FT cells, pCX4bsr, and the anti-NSSB antibody. We also thank A. Morishita and T. Nakamura for technical assistance.

This work was supported by a Grant-in-Aid for Young Scientists (B) from the Ministry of Education, Culture, Sports, Science, and Technology (MEXT), by a Grant-in-Aid for Research on Hepatitis from the Ministry of Health, Labor, and Welfare of Japan, by the Naito Foundation, by the Ichiro Kanehara foundation, and by a research fellowship from the Japan Society for the Promotion of Science (JSPS).

REFERENCES

- Akagi, T., T. Shishido, K. Murata, and H. Hanafusa. 2000. v-Crk activates the phosphoinositide 3-kinase/AKT pathway in transformation. *Proc. Natl. Acad. Sci. USA* 97:7290-7295.
- Ariumi, Y., A. Kaida, M. Hatanaka, and K. Shimotohno. 2001. Functional cross-talk of HIV-1 Tat with p53 through its C-terminal domain. *Biochem. Biophys. Res. Commun.* 287:556-561.
- Ariumi, Y., T. Ego, A. Kaida, M. Matsumoto, P. P. Pandolfi, and K. Shimotohno. 2003. Distinct nuclear body components, PML and SMRT, regulate the *trans*-acting function of HTLV-1 Tax oncoprotein. *Oncogene* 22:1611-1619.
- Ariumi, Y., P. Turelli, M. Masutani, and D. Trono. 2005. DNA damage sensors ATM, ATR, DNA-PKcs, and PARP-1 are dispensable for human immunodeficiency virus type 1 integration. *J. Virol.* 79:2973-2978.
- Bridge, A. J., S. Pebernard, A. Ducraux, A.-L. Nicoulaz, and R. Iggo. 2003. Induction of an interferon response by RNAi vectors in mammalian cells. *Nat. Genet.* 34:263-264.
- Brummelkamp, T. R., R. Bernards, and R. Agami. 2002. A system for stable expression of short interfering RNAs in mammalian cells. *Science* 296:550-553.
- Chang, P. C., C. W. Chi, G. Y. Chau, F. Y. Li, Y. H. Tsai, J. C. Wu, and Y. H. Lee. 2006. DDX3, a DEAD box RNA helicase, is deregulated in hepatitis virus-associated hepatocellular carcinoma and is involved in cell growth control. *Oncogene* 25:1991-2003.
- Chao, C. H., C. M. Chen, P. L. Cheng, J. W. Shih, A. P. Tsou, and Y. H. Lee. 2006. DDX3, a DEAD box RNA helicase with tumor growth-suppressive property and transcriptional regulation activity of the p21^{waf1/cip1} promoter, is a candidate tumor suppressor. *Cancer Res.* 66:6579-6588.
- Cordin, O., J. Banroques, N. K. Tanner, and P. Linder. 2006. The DEAD-box protein family of RNA helicases. *Gene* 367:17-37.
- Fang, J., S. Kubota, B. Yang, N. Zhou, H. Zang, R. Godbout, and R. J. Pomerantz. 2004. A DEAD box protein facilitates HIV-1 replication as a cellular co-factor of Rev. *Virology* 330:471-480.
- Goh, P. Y., Y. J. Tan, S. P. Lim, Y. H. Tan, S. G. Lim, F. Fuller-Pace, and W. Hong. 2004. Cellular RNA helicase p68 relocalization and interaction with the hepatitis C virus (HCV) NS5B protein and the potential role of p68 in HCV RNA replication. *J. Virol.* 78:5288-5298.
- Huang, H., M. L. Shiffman, R. C. Cheung, T. J. Layden, S. Friedman, O. T. Abar, L. Yee, A. P. Chokkalingam, S. J. Schrod, J. Chan, J. J. Catanese, D. U. Leong, D. Ross, X. Hu, A. Monto, L. B. McAllister, S. Broder, T. White, J. J. Smitsky, and T. L. Wright. 2006. Identification of two gene variants associated with risk of advanced fibrosis in patients with chronic hepatitis C. *Gastroenterology* 130:1679-1687.
- Ikeda, M., K. Abe, H. Dansako, T. Nakamura, K. Naka, and N. Kato. 2005. Efficient replication of a full-length hepatitis C virus genome, strain O, in cell culture, and development of a luciferase reporter system. *Biochem. Biophys. Res. Commun.* 329:1350-1359.
- Kato, N., K. Sugiyama, K. Namba, H. Dansako, T. Nakamura, M. Takami,

- K. Naka, A. Nozaki, and K. Shimotohno. 2003. Establishment of a hepatitis C virus subgenomic replicon derived from human hepatocytes infected in vitro. *Biochem. Biophys. Res. Commun.* 306:756–766.
15. Kwong, A. D., B. G. Rao, and K. T. Jeang. 2005. Viral and cellular RNA helicases as antiviral targets. *Nat. Rev. Drug Discov.* 4:845–853.
 16. Lohmann, V., F. Körner, J.-O. Koch, U. Herian, L. Theilmann, and R. Bartenschlager. 1999. Replication of subgenomic hepatitis C virus RNAs in a hepatoma cell line. *Science* 285:110–113.
 17. Mamiya, N., and H. J. Worman. 1999. Hepatitis C virus core protein binds to a DEAD box RNA helicase. *J. Biol. Chem.* 274:15751–15756.
 18. Naldini, L., U. Blömer, P. Gally, D. Ory, R. Mulligan, F. H. Gage, L. M. Verma, and D. Trono. 1996. In vivo gene delivery and stable transduction of non-dividing cells by a lentiviral vector. *Science* 272:263–267.
 19. Owsianka, A. M., and A. H. Patel. 1999. Hepatitis C virus core protein interacts with a human DEAD box protein DDX3. *Virology* 257:330–340.
 20. Rocak, S., and P. Linder. 2004. DEAD-box proteins: the driving forces behind RNA metabolism. *Nat. Rev. Mol. Cell Biol.* 5:232–241.
 21. Sato, S., M. Fukasawa, Y. Yamakawa, T. Natsume, T. Suzuki, I. Shoji, H. Aizaki, T. Miyamura, and M. Nishijima. 2006. Proteomic profiling of lipid droplet proteins in hepatoma cell lines expressing hepatitis C virus core protein. *J. Biochem.* 139:921–930.
 22. Tingting, P., F. Caiyun, Y. Zhigang, Y. Pengyuan, and Y. Zhenghong. 2006. Subproteomic analysis of the cellular proteins associated with the 3' untranslated region of the hepatitis C virus genome in human liver cells. *Biochem. Biophys. Res. Commun.* 347:683–691.
 23. Wakita, T., T. Pietschmann, T. Kato, T. Date, M. Miyamoto, Z. Zhao, K. Murthy, A. Habermann, H. G. Kräusslich, M. Mizokami, R. Bartenschlager, and T. J. Liang. 2005. Production of infectious hepatitis C virus in tissue culture from a cloned viral genome. *Nat. Med.* 11:791–796.
 24. Yedavalli, V. S., C. Neuveut, Y. H. Chi, L. Kleiman, and K. T. Jeang. 2004. Requirement of DDX3 DEAD box RNA helicase for HIV-1 Rev-RRE export function. *Cell* 119:381–392.
 25. You, L. R., C. M. Chen, T. S. Yeh, T. Y. Tsai, R. T. Mai, C. H. Lin, and Y. H. Lee. 1999. Hepatitis C virus core protein interacts with cellular putative RNA helicase. *J. Virol.* 73:2841–2853.
 26. Zufferey, R., D. Nagy, R. J. Mandel, L. Naldini, and D. Trono. 1997. Multiply attenuated lentiviral vector achieves efficient gene delivery in vivo. *Nat. Biotechnol.* 15:871–875.

The lipid droplet is an important organelle for hepatitis C virus production

Yusuke Miyanari^{1,2}, Kimie Atsuzawa³, Nobuteru Usuda³, Koichi Watashi^{1,2}, Takayuki Hishiki^{1,2}, Margarita Zayas⁴, Ralf Bartenschlager⁴, Takaji Wakita⁵, Makoto Hijikata^{1,2} and Kunitada Shimotohno^{1,2,6}

The lipid droplet (LD) is an organelle that is used for the storage of neutral lipids. It dynamically moves through the cytoplasm, interacting with other organelles, including the endoplasmic reticulum (ER)^{1–3}. These interactions are thought to facilitate the transport of lipids and proteins to other organelles. The hepatitis C virus (HCV) is a causative agent of chronic liver diseases⁴. HCV capsid protein (Core) associates with the LD⁵, envelope proteins E1 and E2 reside in the ER lumen⁶, and the viral replicase is assumed to localize on ER-derived membranes. How and where HCV particles are assembled, however, is poorly understood. Here, we show that the LD is involved in the production of infectious virus particles. We demonstrate that Core recruits nonstructural (NS) proteins and replication complexes to LD-associated membranes, and that this recruitment is critical for producing infectious viruses. Furthermore, virus particles were observed in close proximity to LDs, indicating that some steps of virus assembly take place around LDs. This study reveals a novel function of LDs in the assembly of infectious HCV and provides a new perspective on how viruses usurp cellular functions.

Hepatitis C virus (HCV) has a plus-strand RNA genome that encodes the viral structural proteins Core, E1 and E2, the p7, and the nonstructural (NS) proteins 2, 3, 4A, 4B, 5A and 5B (refs 7, 8). NS proteins are reported to localize on the cytoplasmic side of endoplasmic reticulum (ER) membranes⁹. To elucidate the mechanisms of virus production, we used a HCV strain, JFH1, which can produce infectious viruses^{10–12}. We first investigated the subcellular localization of the HCV proteins in cells that had been transfected with JFH1^{E2FL} RNA, in which a part of the hypervariable region 1 of E2 was replaced by the FLAG epitope tag (see Supplementary Information, Fig. S1, S2a–d). Core localized to the lipid droplets (LDs; Fig. 1a), as previously reported⁵. Interestingly, NS proteins were also detected around LDs in 60–90% of JFH1^{E2FL}-replicating cells (Fig. 1a, c). Similar levels of colocalization of LDs with viral proteins were observed in cells that had been transfected with chimeric HCV genomes

expressing structural proteins, p7 and part of NS2 of the genotype 1b (Con1) or the genotype 1a (H77) isolate (see Supplementary Information, Fig. S1, S2e)¹³. In contrast, there was no close association between the LDs and NS proteins in cells that had been transfected with JFH1^{ΔC3} RNA (Fig. 1b, c), which lacked the coding region of Core (Supplementary Information, Fig. S1). NS proteins were diffusely present on the ER, suggesting that NS proteins are translocated from the ER to LDs in JFH1^{E2FL}-replicating cells in a Core-dependent manner. Importantly, there was no association between LDs and PDI, an ER marker protein, indicating that either ER membranes were absent in close proximity to LDs or that PDI was excluded from such membranes (Fig. 1c). These results were supported by western blot analysis of the LD fraction (Fig. 1d). The LD fraction contained ADRP, an LD marker, but not the ER markers Calnexin and Grp78 (data not shown), indicating that there was no ER contamination in the LD fraction. However, the LD fraction from JFH1^{E2FL}-replicating cells contained high levels of viral proteins in contrast to the LD fraction from JFH1^{ΔC3}-replicating cells (in which HCV proteins were virtually absent (Fig. 1d, LD fraction)), even though the expression levels of the NS proteins in whole-cell extracts were similar (Fig. 1d, whole-cell extract). About 20–45% of the total HCV proteins associated with the LDs in JFH1^{E2FL}-replicating cells (Fig. 1e). Consistent with previous reports that Core enhances the formation of LDs¹⁴, overproduction of LDs was observed in JFH1^{E2FL}-, but not JFH1^{ΔC3}-replicating cells (Supplementary Information, Fig. S3a–l). Treatment of the cells with oleic acid, which enhanced the formation of LDs, did not affect either HCV protein levels or the recruitment of viral proteins to LDs in JFH1^{ΔC3}-replicating cells (Supplementary Information, Fig. S3m–p). Thus, the overproduction of LDs is insufficient for the recruitment of HCV proteins to LDs. To examine the ability of Core to recruit NS proteins to LDs, JFH1^{ΔC3}-replicating cells were transfected with a plasmid-expressing Core (Core^{wt}) (Fig. 1f, g). NS5A accumulated around LDs (Fig. 1f, arrowheads and panel 2), as did NS3 and NS4AB (Fig. 1g), in cells expressing Core^{wt}. The translocation of NS proteins to LDs was, however, not observed in JFH1^{ΔC3}-replicating cells expressing Core^{pp7AA} (Fig. 1g and Supplementary Information, Fig. S2f–h),

¹Department of Viral Oncology, Institute for Virus Research, Kyoto University, Kyoto 606-8507, Japan; ²Graduate School of Biostudies, Kyoto University, Kyoto 606-8507, Japan; ³Department of Anatomy, Fujita Health University School of Medicine, Toyoake 470-1192, Japan; ⁴Department of Molecular Virology, University of Heidelberg, 69120 Heidelberg, Germany; ⁵Department of Virology II, National Institute of Infectious Diseases, Tokyo 162-8640, Japan
⁶Correspondence should be addressed to K.S. (e-mail: shimkuni@z8.keio.jp)

Received 16 March 2007; accepted 31 July 2007; published online 26 August 2007; DOI: 10.1038/ncb1631

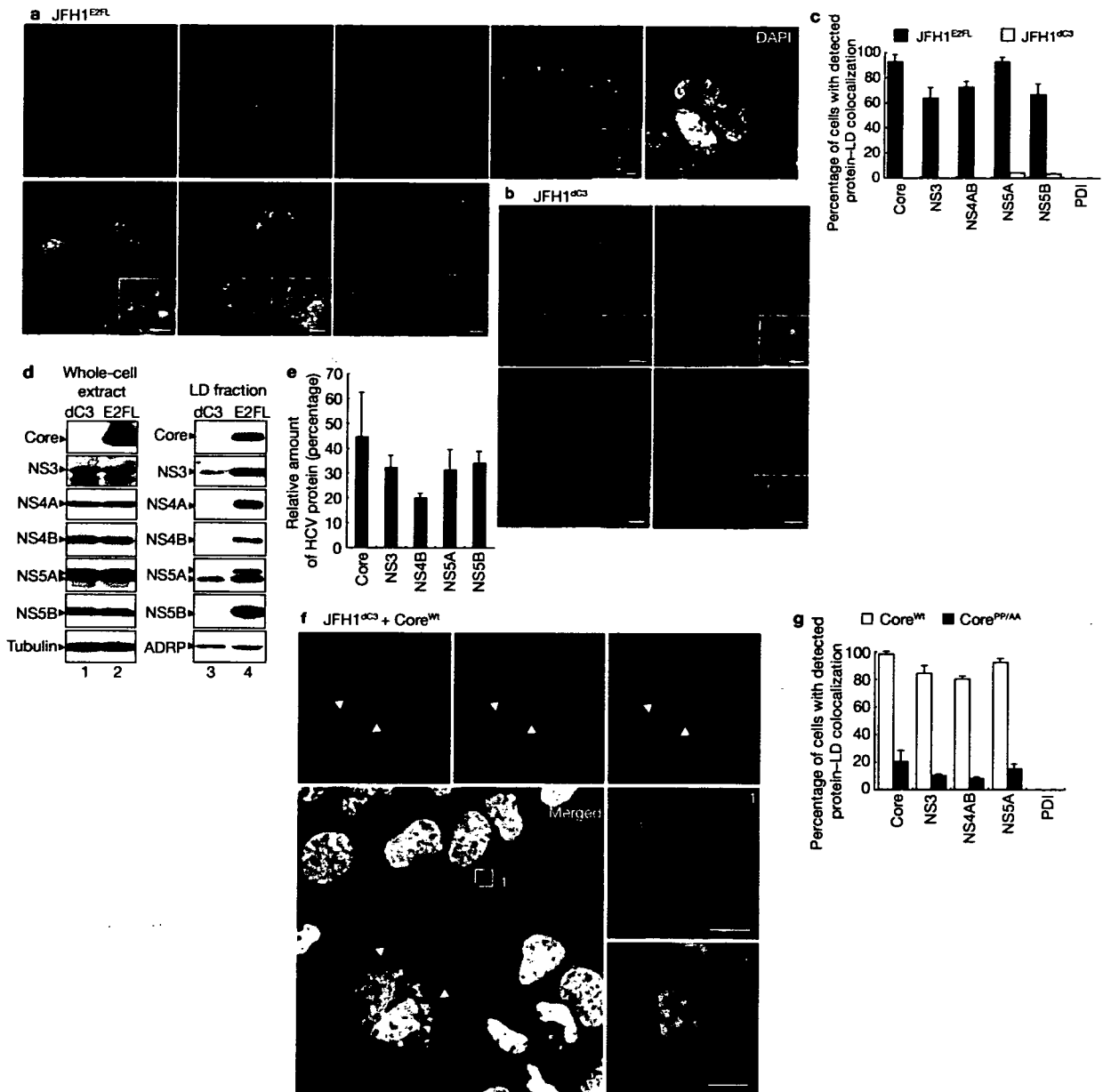


Figure 1 Core recruits NS proteins to LDs. (a) Huh-7 cells transfected with JFH1^{E2FL} RNA were labelled with antibodies against Core (red), NS5A (blue), NS3 (red), NS4AB (red) or NS5B (red). Lipid droplets (LDs) and nuclei were stained with BODIPY 493/503 (green) and DAPI (white in upper panel, blue in lower panels), respectively. Insets are high magnification images of areas in the respective panel. (b) JFH1^{dC3} replicon-bearing cells were labelled with DAPI (blue), BODIPY 493/503 (green) and indicated antibodies (red). The insets are high magnifications of the corresponding panel. (c) Percentages of JFH1^{E2FL}- or JFH1^{dC3}-bearing cells in which hepatitis C virus (HCV) proteins or PDI colocalize with LDs ($n > 200$). (d) Western blot analysis of HCV proteins and marker proteins in whole-cell extracts and the LD fractions from cells transfected with JFH1^{E2FL} (E2FL) or JFH1^{dC3} (dC3) RNA. (e) HCV proteins were quantified by using

western blotting data of the purified LD fraction and whole-cell extracts of JFH1^{E2FL}-replicating cells. Results are shown as relative amounts of HCV proteins co-fractionated with LDs. This results correspond well with results obtained by quantitative immunofluorescence staining (data not shown). (f) Trans-complementation with Core^M relocates NS proteins to LDs. JFH1^{dC3} replicon-bearing cells were transfected with pcDNA3-Core^M and labelled with BODIPY 493/503 (green), DAPI (white) and antibodies against NS5A (red) and Core (blue). Arrowheads indicate Core^M-expressing cells. Higher-magnification images of area 1 and area 2 are shown in panels 1 and 2, respectively. Scale bars, 2 μ m. (g) The percentages of cells in which HCV proteins colocalize with LDs in the presence of Core^M or Core^{PPIA} ($n > 200$). Uncropped images of gels are shown in Supplementary Information Fig. S6. All error bars are derived from s.d.

a variant of Core containing two alanine substitutions at amino-acid positions 138 and 143 that fails to associate with LDs¹⁵. These results show that LD-associated Core recruits NS proteins from the ER to LDs.

Next, we investigated whether Core also recruited HCV RNA to LDs. *In situ* hybridization analysis showed that in more than 80% of JFH1^{E2FL}-replicating cells, both plus- and minus-strand RNAs were diffusely

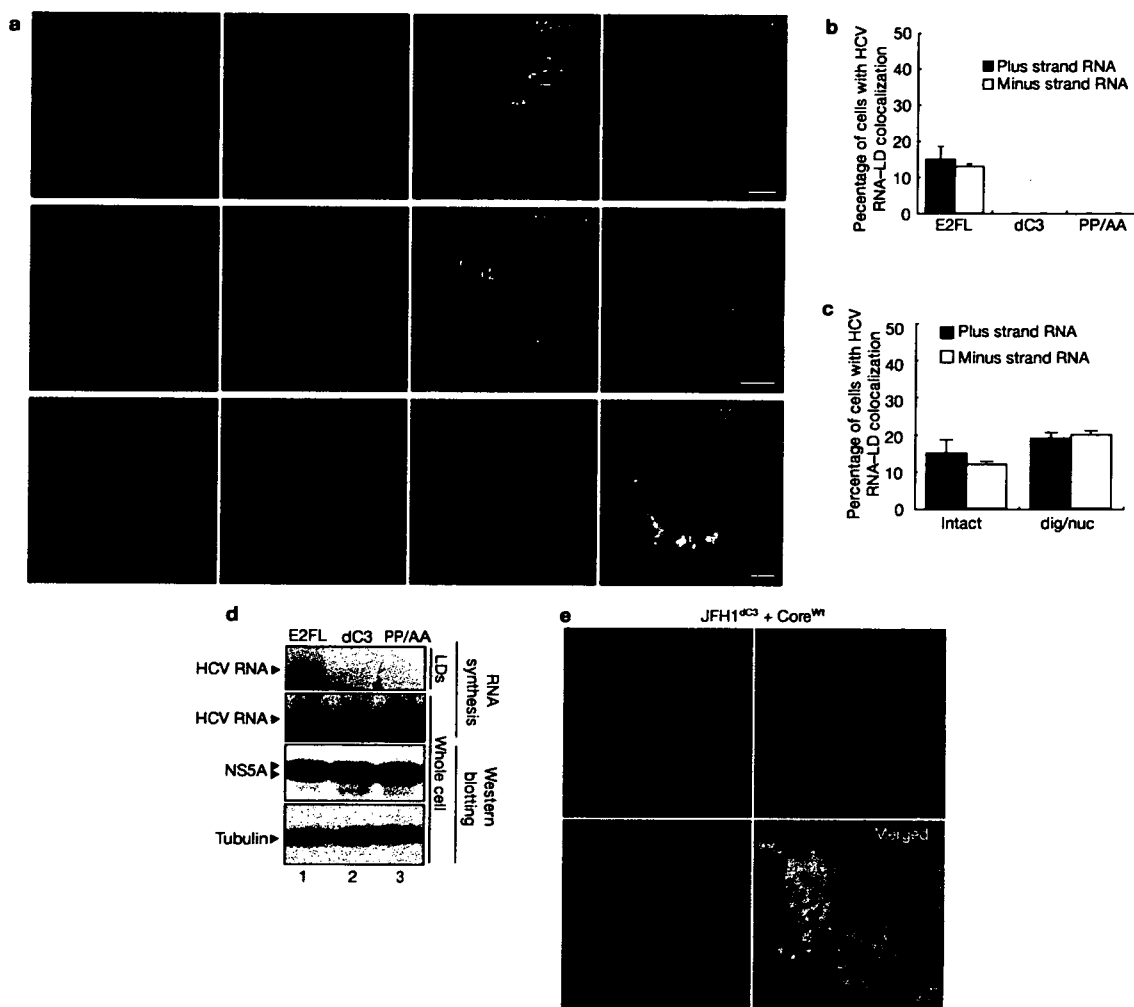


Figure 2 Core-dependent recruitment of active HCV replication complexes to the LD. (a) Huh-7 cells transfected with JFH1^{E2FL} RNA were analysed by *in situ* hybridization with strand-specific probes (plus or minus). The cells were labelled to simultaneously visualize lipid droplets (LDs), NS5A and Core (lower panels). Higher-magnification images of area 1 and area 2 are shown in the upper and middle right panels 1 and 2, respectively. Scale bars: 2 μ m (panels 1, 2); 10 μ m (lower right panel). (b) The percentages of JFH1^{E2FL}-, JFH1^{dC3}- and JFH1^{PP/AA}-expressing cells positive for overlapping signals for LDs and plus- or minus-strand hepatitis C virus (HCV) RNA ($n > 200$). (c) Intact or digitonin and nuclease-treated (dig/nuc) JFH1^{E2FL} replicon-bearing cells were analysed

by *in situ* hybridization. The percentages of cells with overlapping signals for LD and plus- or minus-strand HCV RNA are shown ($n > 200$). (d) RNA-synthesizing activity in the LD fractions purified from cells transfected with JFH1^{E2FL}, JFH1^{dC3} or JFH1^{PP/AA} RNA (top panel). As a control, HCV RNA synthesis activity in digitonin-permeabilized cells was analysed (second panel from the top). HCV protein levels represented by NS5A are shown, together with the level of tubulin (bottom two panels). (e) Localization of plus-strand HCV RNA and Core in JFH1^{dC3} replicon-bearing cells transfected with pcDNA3-Core^{Wt} (Scale bar, 10 μ m). Uncropped images of gels are shown in Supplementary Information Fig. S6. All error bars are derived from s.d.

located in the perinuclear region (see Supplementary Information, Fig. S4a). More importantly, in about 20% of these cells, plus- and minus-strand RNAs accumulated around LDs (Fig. 2a, upper and middle panels; 2b) and colocalized with HCV proteins such as Core and NS5A (Fig. 2a, lower panels). No association between HCV RNA and LDs was detected in JFH1^{dC3}- or JFH1^{PP/AA}-replicating cells (Fig. 2b). Northern blot analysis revealed that 4.8% and 5.4% of total plus- and minus-strand HCV RNA, respectively, were detected in purified LD fractions of JFH1^{E2FL}-replicating cells (data not shown). Induction of LD formation with oleic acid did not affect HCV RNA accumulation around LDs (data not shown). These results provide strong evidence that Core recruits HCV RNA as well as NS proteins to LDs.

The HCV replication complex is compartmentalized by lipid bilayer membranes¹⁶⁻¹⁸. Therefore, HCV RNA in the complex is resistant to nuclease treatment in digitonin-permeabilized cells¹⁷ (Supplementary Information, Fig. S4b-d). *In situ* hybridization analysis did not reveal a significant difference in the number of cells containing LD-associated HCV RNA before and after nuclease treatment (Fig. 2c), indicating that HCV RNA around LDs is part of the replication complex. An RNA synthesis assay showed that the purified LD fraction from JFH1^{E2FL}-, but not JFH1^{dC3}- or JFH1^{PP/AA}-replicating cells, possessed HCV RNA synthesis activity, even though the expression levels of viral proteins and RNA-synthesizing activities in total cell lysates were similar (Fig. 2d). Moreover, the addition of Core^{Wt} rescued the localization of plus- and minus-strand

LETTERS

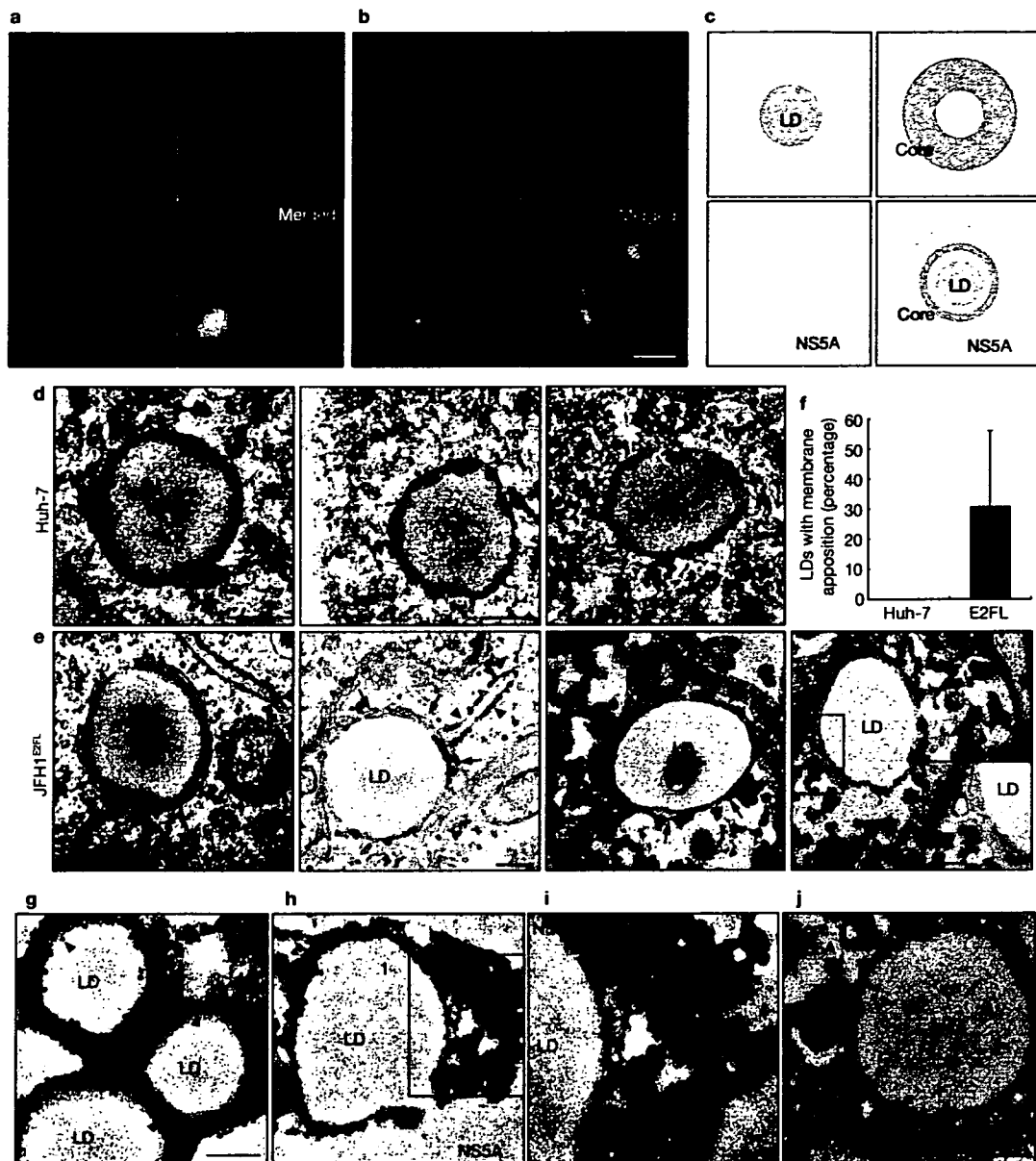


Figure 3 Spatial distribution of Core and NS5A relative to the LD. (a, b) The localizations of Core, NS5A and ADRP around the lipid droplets (LDs) in JFH1^{E2FL} replicon-bearing cells were analysed using immunofluorescence microscopy. Scale bars, 1 μ m. (c) Typical images of the localization of LDs, Core, NS5A and merged images are shown with the relative scale of each image. (d, e) Transmission electron micrographs of LDs in naive Huh-7 cells and JFH1^{E2FL}-expressing cells. Arrows and arrowheads indicate LD-associated membranes and rough ER membranes, respectively. (f) Frequency of LDs with close appositions

of membrane cisternae. About 100 Huh-7 cells or JFH1^{E2FL}-expressing cells, respectively, were chosen randomly. LDs with apposed membrane cisternae, as exemplified in panel e, were counted as positive. The LDs judged as positive were divided by the total number of LDs. (g-j) Immunoelectron micrographs of LDs labelled with antibodies against Core (g), NS5A (h, i) or both (j) are shown. Panel i is a higher magnification of area 1 in panel h. In panel j, Core and NS5A are labelled with 15 nm and 10 nm gold particles, respectively. Scale bars, 200 nm. All error bars are derived from s.d.

HCV RNA around LDs in JFH1^{4C3}-replicating cells (Fig. 2e and data not shown). Both plus- and minus-strand RNA associated with LDs were nuclease resistant (data not shown). These results demonstrate that Core recruits biologically active replication complexes to LDs.

The LD is surrounded by a phospholipid monolayer¹⁹, whereas HCV replication complexes are likely to be surrounded by lipid bilayer membranes^{16,17}. Therefore, the replication complexes might not be directly

associated with the membranes of LDs. To characterize the colocalization of LDs, viral proteins and replication complexes more precisely, we analysed the localization of NS5A with high-resolution immunofluorescence microscopy. Core was completely colocalized with ADRP, residing on the surface of LDs²⁰ (Fig. 3a), thus indicating that Core also directly associates with the surface of LDs. More importantly, NS5A mainly localized around the Core-positive area, resulting in a doughnut-shaped signal with a diameter slightly

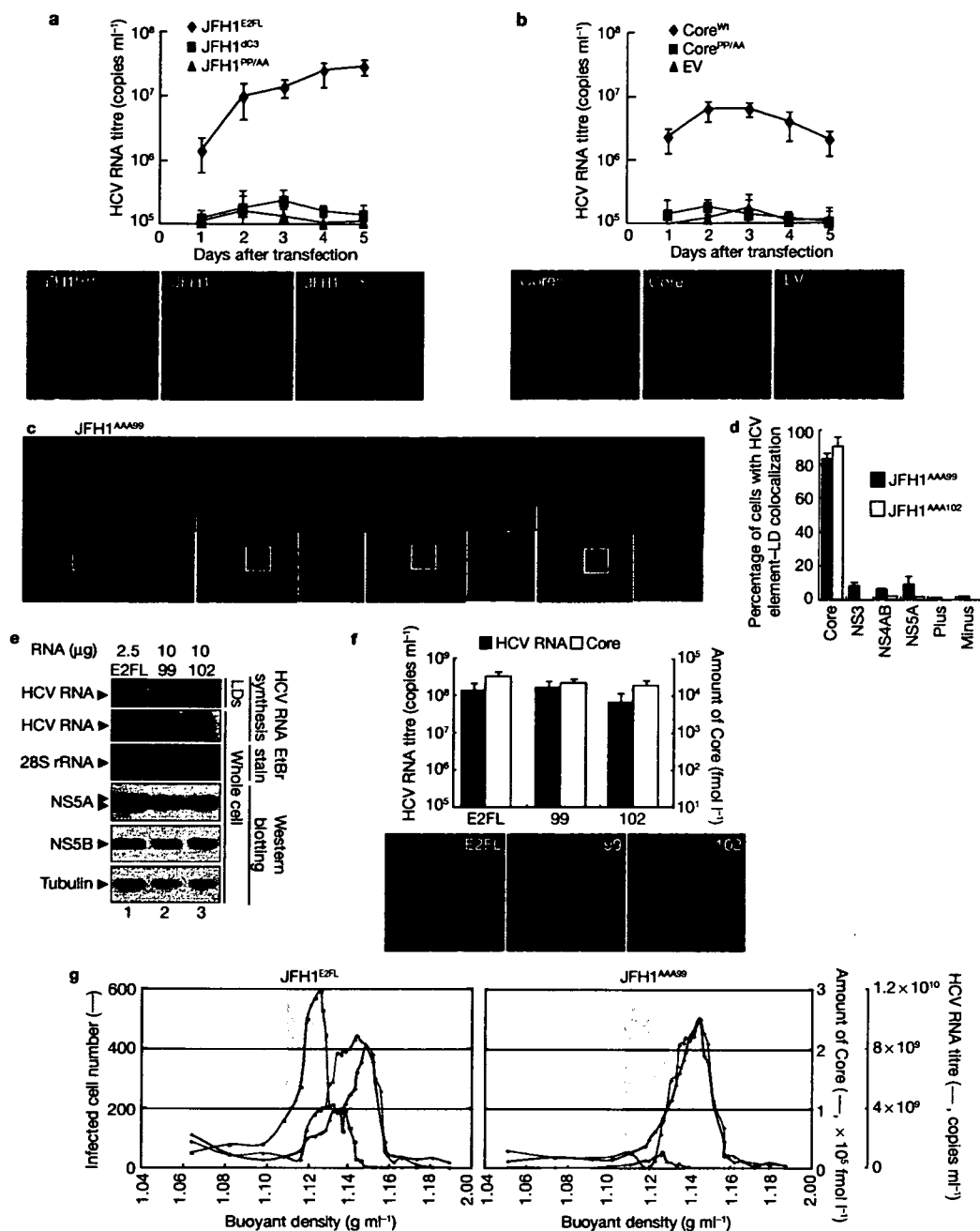


Figure 4 LD associations of Core and NS proteins are necessary for the production of infectious HCV particles. (a) The culture medium from JFH1^{E2FL}-, JFH1^{ΔC3}- or JFH1^{PP1AA}-replicating cells was collected at the indicated time points and the titre of hepatitis C virus (HCV) RNA was measured by real-time RT-PCR (upper panel, $n = 3$). The culture medium was added to naïve Huh7.5 cells and, 24 h after inoculation, and cells were labelled with anti-HCV antibodies (lower panels, red). (b) JFH1^{ΔC3} replicon-bearing cells were transfected with pcDNA3 (EV), pcDNA3-Core^M (Core^M) or pcDNA3-Core^{PP1AA} (Core^{PP1AA}). The level of HCV RNA and the infectivity of the culture medium were examined as described above ($n = 3$). (c) Subcellular localization of NS5A and Core in cells expressing JFH1^{AAA99}. The insets are high magnifications of the area of the corresponding panel. Scale bar, 2 μm . (d) Percentages of cells in which the signals for given HCV proteins, and plus- and minus-strand HCV RNA, overlapped with those for LDs ($n > 200$). (e) Different amounts of JFH1^{E2FL} (E2FL), JFH1^{AAA99} (99) or JFH1^{AAA102} (102) RNAs, respectively, were transfected into the same number of

Huh-7 cells. HCV RNA synthesis activity in purified LD fractions (LD) and whole-cell lysates (whole cell) was analysed (HCV RNA synthesis). 28S rRNA was used as a control. Western blot analysis of NS5A, NS5B and tubulin in cells is also shown. All the RNA samples in the top panel were run on the same gel. (f) Analysis of HCV released from cells expressing JFH1^{E2FL}, JFH1^{AAA99} or JFH1^{AAA102}. HCV RNA titres (black bars) and amounts of Core (white bars) accumulated in the culture medium at 5 d after RNA transfection were measured (upper panel, $n = 3$). Infectivity of the culture medium for naïve Huh-7.5 cells was analysed as described above (lower panels). (g) Concentrated culture medium from JFH1^{E2FL}- and JFH1^{AAA99}-replicating cells was fractionated using 20–50% sucrose density-gradient centrifugation at 100,000 g for 16 h. For each fraction, the amounts of Core (black line), HCV RNA (blue line) and infectivity (represented by infected cell numbers in a well; red line) are plotted against the buoyant density (x -axis) ($n = 3$). Uncropped images of gels are shown in Supplementary Information Fig. S6. All error bars are derived from s.d.

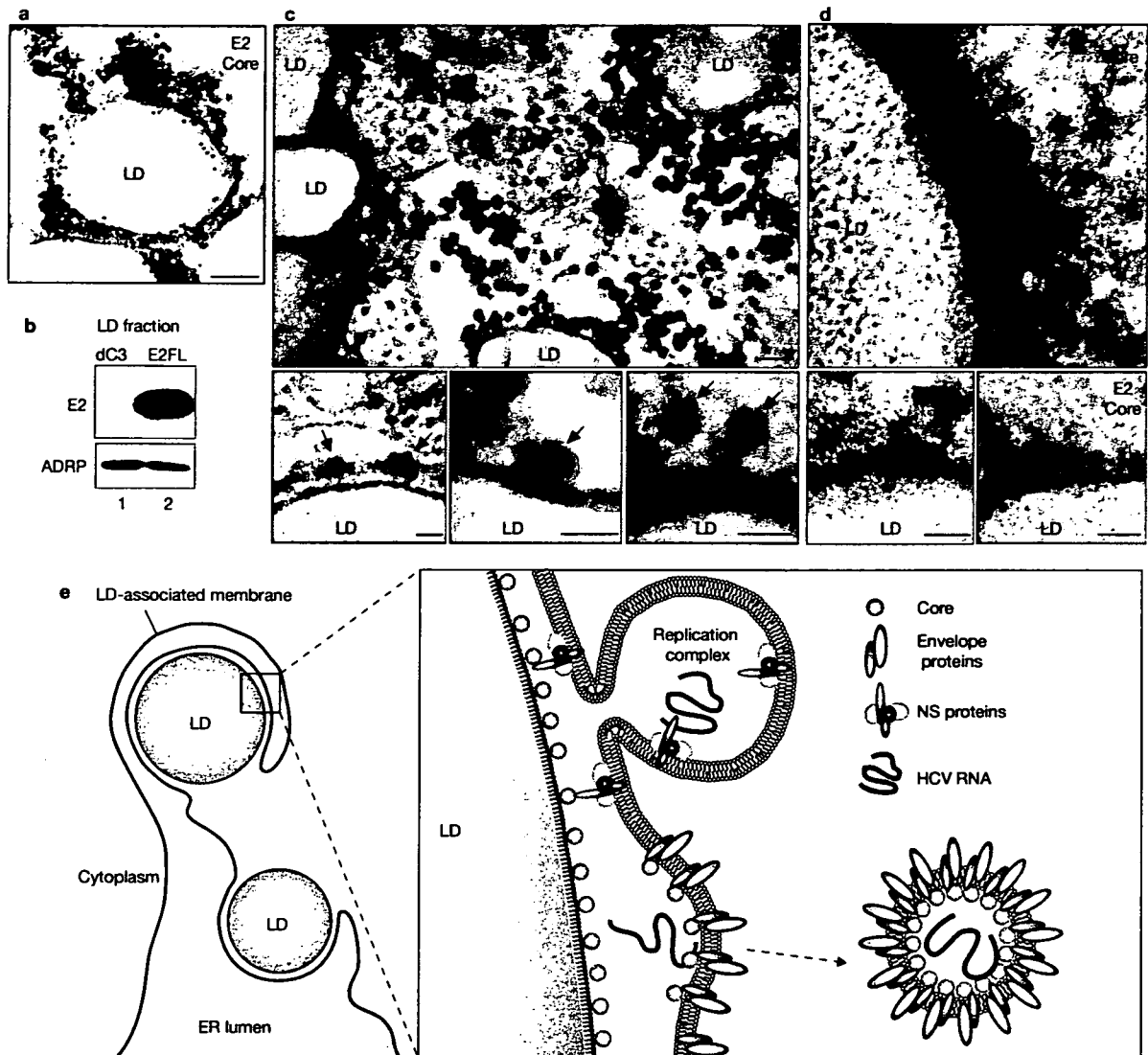


Figure 5 Virus-assembly takes place around the LDs. (a) Immunoelectron microscopic detection of E2 and Core in JFH1^{E2FL}-replicating cells. E2 and Core are labelled with 15 nm and 10 nm gold particles, respectively. (b) Western blot analysis of the lipid droplet (LD) fraction from JFH1^{E2FL} and JFH1^{dC3} replicon-bearing cells with anti-E2 and anti-ADRP antibodies. (c) Transmission electron micrographs of JFH1^{E2FL}-replicating cells. Arrows indicate virus-like particles. (d) Immunoelectron micrographs of LDs labelled with antibodies against Core (10 nm) and E2 (15 nm) are shown. Arrows show Core in electron-dense granules. Scale bar: a and upper panel of c: 100 nm;

in d and lower panels of c: 50 nm. (e) A model for the production of infectious hepatitis C virus (HCV). Core mainly localizes on the monolayer membrane that surrounds the LD. HCV induces the apposition of the LD to the endoplasmic reticulum (ER)-derived bilayer membranes (LD-associated membrane). Core recruits NS proteins, as well as replication complexes, to the LD-associated membrane. NS proteins around the LD can then participate in infectious virus production. E2 also localizes around the LD. Through these associations, virion assembly proceeds in this local environment. Uncropped images of gels are shown in Supplementary Information Fig. S6.

larger than that of Core (Fig. 3b). The LD-proximal NS5A signal partially overlapped with the Core signal (Fig. 3b, c, grey). This concentric staining pattern was also observed with the other NS proteins (Supplementary Information, Fig. S5a), indicating that NS proteins associate with Core on the surface of LDs. Electron microscopic analysis only rarely revealed a close association of LDs with other organelles in naïve Huh-7 cells (Fig. 3d, f). However, in the case of JFH1^{E2FL}-replicating cells, about 30% of the LDs were in close proximity to membrane cisternae (Fig. 3e, arrows; 3f), arguing for a HCV-induced membrane rearrangement around LDs. Core was mainly located on the periphery of LDs, and occasionally signals were

observed in more distal areas of the LDs (Fig. 3g, arrowheads and arrows, respectively). Although some NS5A signals were observed on the surface of the LD, the majority of NS5A signals were detected more distal of LDs (Fig. 3h, i). Furthermore, we often observed membrane cisternae as white lines in the same area as NS5A signals (Fig. 3i, arrows). When the same section was labelled with anti-Core and anti-NS5A antibodies, Core was detected on the surface of the LDs, whereas NS5A was mainly observed in the peripheral area of the LDs (Fig. 3j, arrowheads and arrows, respectively). In summary, these results show that Core recruits NS proteins, as well as HCV replication complexes, to the LD-associated membranes.

The above results prompted us to ask whether Core-LD colocalization is important for the production of infectious virus particles. JFH1^{E2FL}-replicating cells released virions into the culture medium and these viruses were highly infectious for naïve Huh-7.5 cells^{11,21}, although culture medium from JFH1^{PP/AA}- or JFH1^{dC3}-replicating cells did not contain significant levels of HCV RNA and infectious virus (Fig. 4a). However, following trans-complementation with Core^{wt}, a high titre of HCV RNA and infectious virus could be rescued from JFH1^{dC3}-replicating cells (Fig. 4b; and see Supplementary Information, Fig. S5b, c). In contrast, the production of infectious viruses was not rescued by trans-complementation with Core^{PP/AA} (Fig. 4b). RNA-binding properties and oligomerization of Core^{wt} and Core^{PP/AA}, which are both necessary for virus assembly, were similar (Supplementary Information, Fig. S5d; ref. 22), arguing that the primary defect of this mutant in preventing infectious virus production is the inability to associate with LDs.

To investigate the contribution of NS proteins around LDs to infectious virus production, we used variants of NS5A, which were not recruited to LDs even in the presence of Core. We assumed that NS5A was crucial for recruiting other NS proteins to LDs, because the level of NS5A recruited to LDs via Core was higher than the levels of the other recruited NS proteins (Fig. 1c, JFH1^{E2FL}). Using alanine-scanning mutagenesis within the NS5A coding region of JFH1^{E2FL}, we generated two mutants, JFH1^{AAA99} and JFH1^{AAA102}, in which the amino-acid sequence APK (aa 99–101 of NS5A) or PPT (aa 102–104 of NS5A) was replaced by AAA (Supplementary Information, Fig. S1). In JFH1^{AAA99}- and JFH1^{AAA102}-replicating cells, NS5A was rarely detected around LDs, whereas Core was still localized to LDs (Fig. 4c, d). Importantly, these mutations impaired not only the NS5A association with LDs, but also the recruitment of other NS proteins and viral RNAs to LDs (Fig. 4d). These results indicate that NS5A is a key protein that recruits replication complexes to LDs. Importantly, HCV RNA synthesis activity in the LD fractions from these mutant JFH1-replicating cells was also severely impaired (Fig. 4e), corroborating the lack of association of HCV replication complexes with LDs.

To investigate the infectious virus production of these NS5A mutants, we prepared cells expressing similar levels of HCV proteins and RNA by adjusting the amount of transfected HCV RNA (Fig. 4e). This was necessary, because replication activities of these mutants were lower compared with JFH1^{E2FL}. Under these conditions, the amounts of Core and HCV RNA that were released into the culture medium from cells transfected with the mutants were comparable to JFH1^{E2FL} (Fig. 4f, upper graph). However, infectivity titres of the mutants were severely reduced (Fig. 4f, lower panels). In sucrose density-gradient centrifugation of culture medium from JFH1^{E2FL}-bearing cells, two types of HCV particles were detected: low-density particles (about 1.12 g ml⁻¹) with high infectivity (Fig. 4g, green area of JFH1^{E2FL}), and high-density particles (about 1.15 g ml⁻¹) without infectivity (yellow area). This result indicates that only a minor portion of released HCV particles is infectious, whereas the majority of released particles lack infectivity. In contrast, cells bearing the JFH1^{AAA99} mutant almost exclusively released non-infectious particles of around 1.15 g ml⁻¹, whereas infectious particles were barely detectable (Fig. 4g, JFH1^{AAA99}). Taken together, these results provide convincing evidence that the association of NS proteins and replication complexes around LDs is critical for producing infectious viruses, whereas production of non-infectious viruses seems to follow a different pathway.

The results described so far imply that some step(s) of HCV assembly take place around LDs. To explore this possibility, we analysed the distribution of the major envelope protein E2 around the LD. Electron microscopic analysis revealed that, in about 90% of JFH1^{E2FL}-replicating cells, E2 was localized in the peripheral area of the LDs (Fig. 5a, large grains). This labelling pattern was similar to the one observed for NS5A (Fig. 3j), indicating that E2 also localizes on the LD-associated membranes. Western blot analysis of the LD fraction supported this conclusion, because the LD fraction that was purified from JFH1^{E2FL}-replicating cells, but not from JFH1^{dC3}-replicating cells, contained E2 (Fig. 5b). Furthermore, spherical virus-like particles with an average diameter of about 50 nm were observed around LDs in JFH1^{E2FL}-replicating cells (Fig. 5c, upper panel). These particles were never observed in naïve Huh-7 cells. A more refined analysis indicates that these particles are closely associated with membranes in close proximity to LDs (Fig. 5c, lower panels, arrows). Finally, these particles around the LDs reacted with Core- and E2-specific antibodies, arguing that the particles represent true HCV virions (Fig. 5d). These results suggest that infectious HCV particles are generated from the LD-associated membranous environment.

In this study, we have demonstrated that Core recruits NS proteins, HCV RNAs and the replication complex to LD-associated membranes. Mutations of Core and NS5A (Fig. 4), which failed to associate with LDs, impaired the production of infectious virus. We note that the mutant Core retains the ability to interact with RNA (Supplementary Information, Fig. S5b) and to assemble into nucleocapsid²². Similarly, the NS5A mutant still supports viral genome replication and the formation of capsids or virus-like particles, arguing that the introduced mutations in Core and NS5A do not affect overall protein folding, stability or function (Fig. 4). Taken together, the data show that the association of HCV proteins with LDs is important for the production of infectious viral particles (Fig. 5e).

Our results also indicate that NS proteins around the LDs participate in the assembly of infectious virus particles. In one scenario, NS proteins may indirectly contribute to the different steps of virus production — for example, by establishing the microenvironment around the LDs that is required for infectious virus production. Alternatively, NS proteins around the LDs may directly participate in virus production — for example, as components of the replication complex that provide the RNA genome to the assembling nucleocapsid.

In support of the role of LDs in virus formation, we observed that colocalization of HCV protein with LDs was low in cases of the chimera Jc1, supporting up to 1,000-fold higher infectivity titres compared with JFH1 (ref. 13). In a Jc1-infected cell, only about 20% of LDs demonstrated detectable colocalization with Core, but this value increased to 80% in the case of a Jc1 mutant lacking most of the envelope glycoprotein genes and thus being unable to produce infectious virus particles (data not shown). This inverse correlation between the efficiency of virus production and Core protein accumulation on LDs indicates that rapid assembly and virus release results in the rapid liberation of HCV proteins from the LDs.

Steatosis and abnormal lipid metabolism caused by chronic HCV infection may be linked to enhanced LD formation¹⁴. In fact, the overproduction of LDs is induced by Core (Supplementary Information, Fig. S3) and HCV also induces membrane rearrangements around LDs (Fig. 3d–f). Our findings suggest that excessive Core-dependent formation of LDs

LETTERS

and membrane rearrangements are required to supply the necessary microenvironment for virus production. NS proteins and HCV RNA seem to be translocated from the ER to the LD-associated membranes. Interestingly, the LD-associated membranes were occasionally found in continuity with ribosome-studded rough ER (Fig. 3e, arrowheads). Thus, at least parts of the LD-associated membranes are likely to be derived from ER membranes. ER marker proteins, however, were not detected in the LD fraction, suggesting that the LD-associated membrane is characteristically distinct from that of ER membranes.

To our knowledge, this is the first report showing that LDs are required for the formation of infectious virus particles. The fact that capsid protein of the hepatitis G virus also localizes to LDs¹⁵ indicates that LDs might be important for the production of other viruses as well. Our findings demonstrate a novel function of LDs, provide an important step towards elucidating the mechanism of HCV virion production and open new avenues for novel antiviral intervention. □

METHODS

Antibodies. The antibodies used for immunoblotting and immunolabelling were specific for Core (#32-1 and RR8); E2 (AP-33 (ref. 23); 3/11, CBH5 and Flag M2 (Sigma-Aldrich, St Louis, MO); NS3 (R212)¹⁷; NS4A and 4B (PR12); NS5A (NS5ACL1); NS5B (NS5B-6 and JFH1-1)²⁴; ADRP (Progen Biotechnik, Heidelberg, Germany); tubulin (Oncogene Research Products, MA, USA); Grp78 (StressGen, Victoria, Canada); PDI (StressGen); and Calnexin-NT (StressGen). Antibodies specific for Core (#32-1 and RR8), NS3 (R212) and NS4AB (PR12) were gifts from Dr Kohara (The Tokyo Metropolitan Institute of Medical Science, Japan). Anti-E2 antibody (AP-33) was provided by Dr Patel (MRC Virology Unit, UK). Anti-NS5B (NS5B-6) antibody was kindly provided by Dr Fukuya (Osaka University, Japan). Rabbit polyclonal antibodies specific for NS5A were raised against a bacterially expressed GST-NS5A (1-406 aa) fusion protein. In the case of the HCV chimeras Con1/C3 and H77/C3, immunofluorescence analyses were performed by using the following antibodies: Core (C7/50)²⁵, a JFH1 NS3-specific rabbit polyclonal antiserum; NS4B (#86)²⁵; and NS5A (Austral Biologicals, San Ramon, CA).

Indirect immunofluorescence analysis. Indirect immunofluorescence analysis was performed essentially as described previously¹⁷, with slight modifications. Cells transfected with JFH1 RNA were seeded onto a collagen-coated Labtech II 8-well chamber (Nunc, NY, USA). The coating with collagen was performed using rat-tail collagen type I (BD Bioscience, Palo Alto, CA) according to manufacturer's instructions. Three days after seeding, the cells were washed twice with phosphate-buffered saline (PBS; 137 mM NaCl, 2.7 mM KCl, 4.3 mM Na₂HPO₄ and 1.4 mM KH₂PO₄) and fixed with fixation solution (4% paraformaldehyde and 0.15 M sodium cacodylate at pH 7.4) for 15 min at room temperature. After washing with PBS, the cells were permeabilized with 0.05% Triton X-100 in PBS for 15 min at room temperature. For the precise localization of the proteins, the cells were permeabilized with 50 µg ml⁻¹ of digitonin in PBS for 5 min at room temperature²⁶. After incubating the cells with blocking solution (10% fetal bovine serum and 5% bovine serum albumin (BSA) in PBS) for 30 min, the cells were incubated with the primary antibodies. The fluorescent secondary antibodies were Alexa 568- or Alexa 647-conjugated anti-mouse or anti-rabbit IgG antibodies (Invitrogen, Carlsbad, CA). Nuclei were labelled with 4',6-diamidino-2-phenylindole (DAPI). LDs were visualized with BODIPY 493/503 (Invitrogen). Analyses of JFH1 were performed on a Leica SP2 confocal microscope (Leica, Heidelberg, Germany). Analysis of the Con1/C3 and the H77/C3 chimeras was performed in the same way, except that imaging was performed on a Nikon C1 confocal microscope (Nikon, Tokyo, Japan).

Electron microscopy. For conventional electron microscopy, cells cultured in plastic Petri dishes were processed *in situ*. The cells were fixed in 2.5% glutaraldehyde and 0.1 M sodium phosphate (pH 7.4), and then in OsO₄ and 0.1 M sodium phosphate (pH 7.4). The cells were then dehydrated in a graded ethanol series and embedded in an epoxy resin. Ultrathin sections were cut perpendicular to the base of the dish. For immuno-electron microscopy, cells were detached

from the dish with a cell scraper after fixation in 4% paraformaldehyde, 0.1% glutaraldehyde and 0.1 M sodium phosphate (pH 7.4) for 24 h, and washed in 0.1 M lysine, 0.1 M sodium phosphate (pH 7.4) and 0.15 M sodium chloride. After dehydrating the cells in a graded series of cold ethanol, they were embedded in Lowicryl K4M at -20 °C. Ultrathin sections were labelled with primary antibodies and colloidal gold particles (15 nm) conjugated to anti-mouse IgG or anti-rabbit IgG antibodies. For double labelling, colloidal gold particles with different diameters (10 nm and 15 nm) conjugated to anti-mouse IgG or anti-rabbit IgG antibodies were used. Samples were observed after staining with uranyl acetate and lead citrate with a JEM 1010 electron microscope at the accelerating voltage of 80 kV. Anti-Core (#32-1 and RR8), anti-NS5A (NS5ACL1) and anti-E2 (Flag M2) antibodies were used.

Preparation of the lipid droplets. Cells at a confluency of ~80% on a dish with a diameter of 14 cm were scraped in PBS. The cells were pelleted by centrifugation at 1,500 rpm. The pellet was resuspended in 500 µl of hypotonic buffer (50 mM HEPES, 1 mM EDTA and 2 mM MgCl₂ at pH 7.4) supplemented with protease inhibitors (Roche Diagnostics, Basel, Switzerland) and was incubated for 10 min at 4 °C. The suspension was homogenized with 30 strokes of a glass Dounce homogenizer using a tight-fitting pestle. Then, 50 µl of 10× sucrose buffer (0.2 M HEPES, 1.2 M KoAc, 40 mM Mg(oAc)₂ and 50 mM DTT at pH 7.4) was added to the homogenate. The nuclei were removed by centrifugation at 2,000 rpm for 10 min at 4 °C. The supernatant was collected and centrifuged at 16,000 g for 10 min at 4 °C. The supernatant (S16) was mixed with an equal volume of 1.04 M sucrose in isotonic buffer (50 mM HEPES, 100 mM KCl, 2 mM MgCl₂ and protease inhibitors). The solution was set at the bottom of 2.2-ml ultracentrifuge tube (Hitachi Koki, Tokyo, Japan). One milliliter of isotonic buffer was loaded onto the sucrose mixture. The tube was centrifuged at 100,000 g in an S55S rotor (Hitachi Koki) for 30 min at 4 °C. After the centrifugation, the LD fraction on the top of the gradient solution was recovered in isotonic buffer. The suspension was mixed with 1.04 M sucrose and centrifuged again at 100,000 g, as described above, to eliminate possible contamination with other organelles. The collected LD fraction was used for western blotting or the HCV RNA synthesis assay.

HCV RNA synthesis assay. An assay of HCV RNA synthesis using digitonin-permeabilized cells was performed as described previously¹⁷. For RNA synthesis assays using the LD fraction, the LD fraction collected by sucrose-gradient sedimentation was suspended in buffer B, which contained 2 mM manganese (II) chloride, 1 mg ml⁻¹ acetylated BSA (Nacalai Tesque, Kyoto, Japan), 5 mM phosphocreatine (Sigma), 20 units/ml creatine phosphokinase (Sigma), 50 µg ml⁻¹ actinomycin D, 500 µM ATP, 500 µM CTP, 500 µM GTP (Roche Diagnostics) and 1.85 MBq of [α -³²P] UTP (GE Healthcare, Little Chalfont, UK), and incubated at 27 °C for 4 h. The reaction products were analysed by gel electrophoresis followed by autoradiography.

Note: Supplementary Information is available on the Nature Cell Biology website.

ACKNOWLEDGEMENTS

We thank T. Fujimoto and Y. Ohsaki at Nagoya University for helpful discussions and technical assistance. Y.M. is a recipient of a JSPS fellowship. K.S. is supported by Grants-in-Aid for cancer research and for the second-term comprehensive 10-year strategy for cancer control from the Ministry of Health, Labour and Welfare, as well as by a Grant-in-Aid for Scientific Research on Priority Areas "Integrative Research Toward the Conquest of Cancer" from the Ministry of Education, Culture, Sports, Science and Technology of Japan. T.W. is also supported, in part, by a Grant-in-Aid for Scientific Research from the Japan Society for the Promotion of Science; and by the Research on Health Sciences Focusing on Drug Innovation from the Japan Health Sciences Foundation. R.B. is supported by the Sonderforschungsbereich 638 (Teilprojekt A5) and the Deutsche Forschungsgemeinschaft (BA1505/2-1). M.Z. and R.B. thank the Nikon Imaging Center at the University of Heidelberg for providing access to their confocal fluorescence microscopes and Ulrike Engel for the excellent support.

AUTHOR CONTRIBUTIONS

Y.M. and K.S. planned experiments and analyses. Y.M. was responsible for experiments for Figs 1, 2, 3a-c, 4a-e and 5b. K.A., N.U., electron microscopy; T.H., Fig. 1e; M.Z., R.B., Fig. S2e; and K.S. and K.W., Fig. 4f-g. T.W. provided JFH1 strain. Y.M. and K.S. wrote the manuscript. All authors discussed the results and commented on the manuscript.

COMPETING FINANCIAL INTERESTS

The authors declare no competing financial interests.

Published online at <http://www.nature.com/naturecellbiology/>

Reprints and permissions information is available online at <http://npg.nature.com/reprintsandpermissions/>

- Martin, S. & Parton, R. G. Lipid droplets: a unified view of a dynamic organelle. *Nature Rev. Mol. Cell Biol.* **7**, 373–378 (2006).
- Blanchette-Mackie, E. J. *et al.* Perilipin is located on the surface layer of intracellular lipid droplets in adipocytes. *J. Lipid Res.* **36**, 1211–1226 (1995).
- Vock, R. *et al.* Design of the oxygen and substrate pathways. VI. structural basis of intracellular substrate supply to mitochondria in muscle cells. *J. Exp. Biol.* **199**, 1689–1697 (1996).
- Liang, T. J. *et al.* Viral pathogenesis of hepatocellular carcinoma in the United States. *Hepatology* **18**, 1326–1333 (1993).
- Moradpour, D., Englert, C., Wakita, T. & Wands, J. R. Characterization of cell lines allowing tightly regulated expression of hepatitis C virus core protein. *Virology* **222**, 51–63 (1996).
- Deleersnyder, V. *et al.* Formation of native hepatitis C virus glycoprotein complexes. *J. Virol.* **71**, 697–704 (1997).
- Kato, N. *et al.* Molecular cloning of the human hepatitis C virus genome from Japanese patients with non-A, non-B hepatitis. *Proc. Natl Acad. Sci. USA* **87**, 9524–9528 (1990).
- Hijikata, M. & Shimotohno, K. [Mechanisms of hepatitis C viral polyprotein processing]. *Uirusu* **43**, 293–298 (1993).
- Dubuisson, J., Penin, F. & Moradpour, D. Interaction of hepatitis C virus proteins with host cell membranes and lipids. *Trends Cell Biol.* **12**, 517–523 (2002).
- Wakita, T. *et al.* Production of infectious hepatitis C virus in tissue culture from a cloned viral genome. *Nature Med.* **11**, 791–796 (2005).
- Lindenbach, B. D. *et al.* Complete replication of hepatitis C virus in cell culture. *Science* **309**, 623–626 (2005).
- Zhong, J. *et al.* Robust hepatitis C virus infection in vitro. *Proc. Natl Acad. Sci. USA* **102**, 9294–9299 (2005).
- Pietschmann, T. *et al.* Construction and characterization of infectious intragenotypic and intergenotypic hepatitis C virus chimeras. *Proc. Natl Acad. Sci. USA* **103**, 7408–7413 (2006).
- Moriya, K. *et al.* Hepatitis C virus core protein induces hepatic steatosis in transgenic mice. *J. Gen. Virol.* **78**, 1527–1531 (1997).
- Hope, R. G., Murphy, D. J. & McLauchlan, J. The domains required to direct core proteins of hepatitis C virus and GB virus-B to lipid droplets share common features with plant oleosin proteins. *J. Biol. Chem.* **277**, 4261–4270 (2002).
- Egger, D. *et al.* Expression of hepatitis C virus proteins induces distinct membrane alterations including a candidate viral replication complex. *J. Virol.* **76**, 5974–5984 (2002).
- Miyanari, Y. *et al.* Hepatitis C virus non-structural proteins in the probable membranous compartment function in viral genome replication. *J. Biol. Chem.* **278**, 50301–50308 (2003).
- Quinkert, D., Bartenschlager, R. & Lohmann, V. Quantitative analysis of the hepatitis C virus replication complex. *J. Virol.* **79**, 13594–13605 (2005).
- Tauchi-Sato, K., Ozeki, S., Houjou, T., Taguchi, R. & Fujimoto, T. The surface of lipid droplets is a phospholipid monolayer with a unique fatty acid composition. *J. Biol. Chem.* **277**, 44507–44512 (2002).
- Londos, C., Brasaemle, D. L., Schultz, C. J., Segrest, J. P. & Kimmel, A. R. Perilipins, ADRP, and other proteins that associate with intracellular neutral lipid droplets in animal cells. *Semin. Cell Dev. Biol.* **10**, 51–58 (1999).
- Blight, K. J., McKeating, J. A. & Rice, C. M. Highly permissive cell lines for subgenomic and genomic hepatitis C virus RNA replication. *J. Virol.* **76**, 13001–13014 (2002).
- Klein, K. C., Dellos, S. R. & Lingappa, J. R. Identification of residues in the hepatitis C virus core protein that are critical for capsid assembly in a cell-free system. *J. Virol.* **79**, 6814–6826 (2005).
- Owsianka, A. *et al.* Monoclonal antibody AP33 defines a broadly neutralizing epitope on the hepatitis C virus E2 envelope glycoprotein. *J. Virol.* **79**, 11095–11104 (2005).
- Ishii, N. *et al.* Diverse effects of cyclosporine on hepatitis C virus strain replication. *J. Virol.* **80**, 4510–4520 (2006).
- Lohmann, V., Korner, F., Herian, U. & Bartenschlager, R. Biochemical properties of hepatitis C virus NS5B RNA-dependent RNA polymerase and identification of amino acid sequence motifs essential for enzymatic activity. *J. Virol.* **71**, 8416–8428 (1997).
- Ohsaki, Y., Maeda, T. & Fujimoto, T. Fixation and permeabilization protocol is critical for the immunolabeling of lipid droplet proteins. *Histochem. Cell Biol.* **124**, 445–452 (2005).